Marine Physical Laboratory

Ambiguity Surface Manifestation of Downslope Converted Noise Sources

Jean-Marie Q.D. Tran and W.S. Hodgkiss

Supported by the
Office of Naval Research
Grant N00014-91-J-1237

MPL Technical Memorandum 435

MPL-U-12/94
January 1994

Approved for public release; distribution is unlimited.

University of California, San Diego
Scripps Institution of Oceanography

REPORT DOCUMENTATION PAGE

Form Approved OMB No. 0704-0188

1. Agency Use Only (Leave Blank).

2. Report Date. January 1994

3. Report Type and Dates Covered. MPL Technical Memorandum

4. Title and Subtitle.

Ambiguity Surface Manifestation of Downslope Converted Noise Sources

5. Funding Numbers.

N00014-91-J-1237

Project No.
Task No.

6. Author(s).

Jean-Marie Q.D. Tran and W.S. Hodgkiss

7. Performing Monitoring Agency Names(s) and Address(es).

University of California, San Diego
Marine Physical Laboratory
Scripps Institution of Oceanography
San Diego, California 92152-5000

Accesion For
NTIS CRA&I ☒
DTIC TAB ☐
Unannounced ☐
Justification

8. Performing Organization Report Number.

MPL TM-435
MPL-U-12/94

9. Sponsoring/Monitoring Agency Name(s) and Address(es).

Chief of Naval Research
Ballston Tower One
800 North Quincy Street
Arlington, VA 22217-5660 (Code 3240A)

By
Distribution /
Availability Codes
Dist | Avail and / or Special
A-1

10. Sponsoring/Monitoring Agency Report Number.

11. Supplementary Notes.

12a. Distribution/Availability Statement.

Approved for public release; distribution is unlimited.

12b. Distribution Code.

13. Abstract (Maximum 200 words).

This report deals with the manifestation of downslope converted continental shelf noise sources in the matched-field processor (MFP) ambiguity surface. Of interest here is how noise sources outside the range of interest leak into the ambiguity surface through the sidelobe structure of the effective MFP beam (or cell) pattern. The focus is on the appearance of the matched-field processing ambiguity surface due to continental shelf noise, primarily ships, that gets coupled in the deep sound channel. This study is carried out with simulations using the parabolic equation (PE) model. PE is used to simulate the pressure field across a receiving vertical line array in deep water (4000m), 1750 km from the continental shelf.

14. Subject Terms.

Downslope conversion, continental shelf noises, matched field processor.

15. Number of Pages. 38

16. Price Code.

17. Security Classification of Report.	18. Security Classification of This Page.	19. Security Classification of Abstract..	20. Limitation of Abstract.
Unclassified	Unclassified	Unclassified	None

Ambiguity Surface Manifestation of Downslope Converted Noise Sources

Jean-Marie Q.D. Tran and W. S. Hodgkiss

Marine Physical Laboratory

Scripps Institution of Oceanography

San Diego, CA 92152-6400

Abstract

This report deals with the manifestation of downslope converted continental shelf noise sources in the matched-field processor (MFP) ambiguity surface. Of interest here is how noise sources outside the range of interest leak into the ambiguity surface through the sidelobe structure of the effective MFP beam (or cell) pattern. The focus is on the appearance of the matched-field processing ambiguity surface due to continental shelf noise, primarily ships, that gets coupled in the deep sound channel. This study is carried out with simulations using the parabolic equation (PE) model. PE is used to simulate the pressure field across a receiving vertical line array in deep water (4000 m), 1750 km from the continental shelf. A shallow, low frequency (18 Hz) source is assumed deployed at various locations on the continental slope. The MFP ambiguity surfaces are calculated on a search window extending in range across 500 km and in depth down to 1000 m, and obtained with a 1000 m or a 4000 m long simulated receiving array. Shallow sources on the slope show up in the MFP ambiguity surface as deep peaks when downslope conversion takes place. Shallow sources at locations on the slope or in deep water adjacent to the slope where downslope conversion does not take place, appear in the MFP ambiguity surface as shallow sources.

1. Introduction

This report deals with the manifestation of downslope converted continental shelf noise sources in the matched-field processor (MFP) ambiguity surface.

Downslope conversion of acoustic energy has been suggested as one mechanism by which noise radiated by ships or storms gets coupled into the sound channel. Various experiments have been designed to better understand downslope conversion, such as the one conducted by the Marine Physical Laboratory (MPL) in July 1989 in the region of the continental margin NW of Pt Conception, California [1].

Measurements of propagation loss show that bathymetry does strongly influence the propagation of sound from a shallow source and downslope enhancements of up to 10 dB were observed at a deep receiver for sources near the edge of the continental shelf [2-4]. Downslope conversion also provides an explanation for the vertical directionality of low frequency ambient noise in the deep ocean [5-6]. The grazing angle of acoustic rays propagating upon a sloping bottom are reduced by two times the slope angle upon refection. Hence, a shallow source on the continental shelf produces arrivals in deep water with low angles [7]. At long distance, this downslope converted energy is seen as a large contribution to the ambient noise level arriving near the horizontal [5,6,8].

To complement observations of downslope conversion with transmission loss and conventional beamforming results, this report deals with the manifestation of downslope converted continental shelf noise sources in matched-field processing (MFP) ambiguity surfaces. Matched-field processing is a generalized beamforming technique which correlates the field observed by an array of receivers with the predicted field due to a source in a particular range and depth cell. Of interest here is the ambiguity surface contribution due to a noise source outside the range-depth search window, in the continental shelf region, which leaks through the sidelobes of the MFP "beam" steered on a particular hypothesized source location in deep water.

The work performed and presented in this document deals with point source simulations only. The range dependent Parabolic Equation (PE) model [9-11] is used to simulate pressure fields observed at a vertical line array due to low frequency sources placed at various positions on the continental slope as in [8]. PE is also used to compute the set of MFP replica vectors, i.e. the predicted pressure across the array for point sources in a range-depth search window. The geometry and environmental information used in these simulations are similar to those encountered during the MPL Downslope Conversion Experiment [1].

2. Description of the Simulations

The overall propagation geometry is given in Fig. 1. The array of receivers is assumed deployed at a fixed location in deep water (nominal depth of 4000 m). The substantial amount of environmental data, collected during the actual experiment [12] (such as CTDs, XBTs, range varying temperature field obtained with AXBTs), allows the use of a realistic range dependent sound speed structure from the array to the continental slope in this simulation study. Together with the bathymetry, the sound speed field is plotted in Fig. 2 for the deep water and in Fig. 3 for the slope area.

The first deep water environmental sector starts from the receivers and is 30 km wide. It is followed by 27 other deep water sectors (which are 60 km wide), to the continental slope. The deep water sectors have a nominal water depth of 4000 m. The transition from deep water to the continental shelf begins with a gentle 0.4 deg slope for 57.5 km, followed by a sharp rise over 8.8 km from a depth of 3600 m to a depth of 1800 m. This steep slope is followed by a small 2.8 deg slope and a shelf with a depth of 480 m.

The sound speed field is strongly range dependent and Fig. 2 clearly shows the shoaling of the sound axis towards the continental shelf. The geoacoustic model for the 28 deep water sectors corresponds to a fairly reflecting bottom where the 350 m thick sediment layer has a sound speed increasing from 1523.6 m/s, the bottom water sound speed,

to 3500 m/s. The density is 2 g/cm^3 and the attenuation is 0.113 dB/wavelength. These parameters attempt to simulate an abyssal plain with a very thin sediment layer on top of hard basalt. The two wavelength thick PE subbottom has the same properties as the sediments with a sound speed equal to 3500 m/s.

The bottom sound speed profiles in the continental slope area are given in Fig. 4. The shallow water sector sediment layer has a density of 1.5 g/cm^3, and an attenuation of 0.113 dB/wavelength. The steep slope sector starting at -33.7 km in Fig. 3 is assumed to have no sediment deposits and the sound speed is constant equal to 2500 m/s, the density is 2 g/cm^3, the attenuation 0.113 dB/wavelength. The gentle slope sector starting at -42.5 km in Fig. 3 has a density equal to 1.5 g/cm^3 and an attenuation of 0.113 dB/wavelength.

An 18 Hz source is assumed deployed at shallow depth, at four different locations around the continental slope. The source is first on the continental shelf in shallow water (480 m), 1750 km from the receivers (at range 0 in Fig. 3). It is then moved in the middle of the small 2.8 deg. slope, 1729.6 km from the array (at range -20.4 km in Fig. 3). The third station corresponds to the middle of the steep 11.5 deg. slope sector, 1711.9 km from the array (in Fig. 3 at range -38.1 km). Finally, the source is set at the beginning of the gentle 0.4 deg slope sector, 1707.5 km from the fixed receivers (in Fig. 3 at range -42.5 km).

The modified wide angle PE model [10] is run with a 1024 point transform (the sampling in depth is on the order of 6.17 m). The range step is 100 m, close to a wavelength at 18 Hz. The starting field of a source set at a depth of 45 m (approximately half a wavelength at 18 Hz) is used to simulate a ship and is calculated with the normal mode model KRAKEN [13]. The receiving array is assumed fixed in range with respect to the environment, while the source is moved from the shallow water station to the deep water. Two vertical line arrays are considered :

(1) an aperture on the order of 1000 m, deployed from 400 to 1390 m with 80 hydrophones equally spaced every 12.353 m,

(2) a 4000 m aperture covering the full water column with 323 sensors spaced every 12.353 m.

3. Modeling Results

In this section, the simulated data are studied and their physical validity verified. This is carried out by looking at transmission loss and field plots, as well as conventional beamforming results.

First, the existence of the downslope enhancement effect is verified. Fig. 5 gives the transmission loss curves for a 1000 m receiver, as a function of range for the four stations. The range origin in Fig. 5 corresponds to the source in shallow water. The receiving array is 1750 km away. The three other simulated stations have increasing ranges equal to 20.4 km (small 2.8 deg slope), 38.1 km (the steep 11.5 deg slope) and 42.5 km (the beginning of the gentle slope) from the shallow water station. The smallest transmission loss at the array range (top curve in Fig. 5), which is on the order of 100 dB, corresponds to the source in the middle of the small (2.8 deg) slope sector. The next smallest transmission loss at the array range (1750 km), on the order of 105 dB, corresponds to the source in shallow water. The largest transmission losses (107-108 dB) occur when the source is above the steep slope or at the beginning of the gentle slope. Downslope enhancement is therefore observed with levels on the order of 8 dB, consistent with enhancement reported in the literature of up 10 dB [2-4].

These preliminary results indicate that slope interaction happens when the source is either in shallow water or above the small 2.8 deg. slope. A convenient way to verify this conclusion is to look at field plots for the four different simulated transmission experiments. Field plots extending in depth to 4350 m (hence covering the whole water column and the 350 m thick sediment layer as well) and extending in range up to 150 km from the source are given in Figs. 6, 8, 10 and 12 for the four stations while the corresponding bathymetry is given in Figs. 7, 9, 11, 13. Slope interaction and energy

conversion from steep to near horizontal paths are clearly observed for the source in shallow water in Fig. 6 and above the small slope area in Fig. 8. Higher levels are observed in the latter case. On the other hand, there is no slope interaction when the source is above the steep slope or at the beginning of the gentle slope. The corresponding field plots in Figs. 10 and 12 show steep bottom interacting-surface reflected paths occurring every 50 km, forming the usual convergence zone pattern observed for shallow sources in deep water.

The vertical directionality of the field received at the array also can be used to observe the effect of downslope conversion. The results of conventional FFT beamforming on the 1000 m aperture, given in Fig. 14, clearly shows downslope conversion when the source is either in shallow water or above the small 2.8 deg slope. Significant power levels are observed at low angles (within ± 10 deg.). There is no power at low arrival angle observed in the vertical directionality when the source is above the steep slope or at the beginning of the gentle slope. In those two cases, the vertical directionality corresponds to a shallow source in deep water.

The beamforming results obtained with the full water column aperture and given in Fig. 15, are much more difficult to interpret, since actual arrivals are curved rather than planar over the large spatial extent of the vertical line array [14]. The refraction index causes an arrival to have an angle varying locally as a function of depth, according to Snell's law. In such conditions, low angle arrivals can be observed, even for a shallow source in deep water, as in the vertical directionality plot of the the source above the steep slope sector. The arrival structure is highly dependent on the range between the source and the receiving array. When the source is at the beginning of the gentle slope, there is no strong near horizontal arrival. But, when the source is in shallow water or above the small 2.8 deg slope, there is significant power near horizontal in the vertical directionality structure, as expected.

4. Matched-Field Processing Results

Matched-field processing now is used to study the effect of downslope conversion and complement the results presented in the earlier sections. The PE model is used to create the set of replica vectors for a search window extending from 25 to 525 km in range and from 5 to 985 m in depth. The MFP range-depth cells are 2 km wide and 20 m deep. The range step has been chosen relatively large in order to limit the number of PE runs. It does not need to be significantly smaller since the interest in this study is the sidelobe leakage into a deep water MFP cell from shallow sources in the continental slope area.

For each source range, PE is run with an updated input file to correctly account for the range dependence of the environment. The array is assumed fixed and the motion of the source changes the source to receiver range as well as the environmental sector starting ranges. Over the 525 km range extent of interest, there are ten sectors with different sound speed profiles. In order to be consistent with the pressure fields calculated earlier to simulate a source on the continental slope, PE is started with an initial field produced by the normal mode model KRAKEN, even in the case of deep sources.

The MFP ambiguity surfaces displayed in gray-level correspond to the correlation measure given by

$$C(r_s,z_s) = |\mathbf{e}_d^H \mathbf{e}_e|^2 \tag{1}$$

Or in dB :

$$P(r_s,z_s) = 10 \log |\mathbf{e}_d{}^H \mathbf{e}_r|^2 \tag{2}$$

where $\mathbf{e}_d$ corresponds to the simulated data across the vertical line array (due to the shallow source in the continental slope area), normalized to unit norm, and $\mathbf{e}_r$ is the unit norm replica vector which is a function of the hypothesized source range and depth r_s and z_s. H denotes the Hermitian (conjugate transpose) operator. This correlation measure actually is a measure of mismatch between the simulated data and the replica vectors.

4.1. Processing the 1000 m Aperture

The processing results on the 1000 m array with 80 sensors are examined first. The ambiguity surface for the source in shallow water, given in Fig. 16, has peaks forming patterns reminiscent of a source at depth. These features happen especially in the 275-525 km region. They appear centered around a depth of 300 m and have a convergence zone periodicity on the order of 50 to 60 km. Hence, Fig. 16 shows that the shallow source, located on the shelf in shallow water, 1750 km from the receiving array, looks like a deep source in the MFP range-depth search window. When the source is above the small 2.8 deg. slope, the slope conversion is even stronger. In this case, the ambiguity surface gray-level displayed in Fig. 17, has the same character as Fig. 16, with even broader peaks distributed in depth primarily around 300 m and 600 m. A convergence zone periodicity also is observed. The shallow source above the small 2.8 deg. slope does also look like a deep source in the MFP search window.

The ambiguity surfaces for the source above the steep slopeand at the beginning of the gentle slope are given in Figs. 18 and 19. Both surfaces are characterized by sets of peaks at shallow depths, around 100 m. These surfaces have a character very much different from the two slope interacting source stations. They have strong peaks at shallower depth, but none deeper. The shallow water sources in the continental rise area (where there is no downslope conversion), 1700 km from the array, look like shallow sources in the MFP search window.

To help interpret the results, the beamforming and matched-field processing results are examined for two sources located within the MFP search window at a range of 423 km and at two different depths : 45 m and 305 m depth. The angular spectra obtained with the 1000 m array for the two source depths are given in Fig. 20. The deeper source produces strong horizontal arrivals, while the shallow source does not. The MFP ambiguity surfaces are gray-level displayed in Figs. 21 and 22. The ambiguity surface of the shallow

source is characterized by small peaks distributed at shallower depths with a convergence zone periodicity in range. It is similar to the surfaces where the source is at the beginning of the gentle slope (Fig. 18), or in the middle of the steep sector area (Fig. 19). On the other hand, the ambiguity surface of the deeper source produces butterfly patterns with peaks distributed at great depth, similar to the ambiguity surfaces of the slope interacting stations.

The appearance of the MFP ambiguity surface is very different whether or not there is downslope conversion, as the initial transmission loss and conventional beamforming results suggested. The shoaling of the sound axis seems to have little effect on the coupling of sound in the deep sound channel for these low frequency simulations and this particular array configuration. This is consistent with the conventional beamforming results.

The location of the highest peak in the ambiguity surfaces and the corresponding squared correlation values (Eq. (1)), are given in Table 1. The highest peak is deeper when there is downslope enhancement than when there is not. The observed correlation values are high, above 0.6 with the maximum value observed when slope conversion is largest (i.e. when the source is above the small 2.8 deg. slope sector).

4.2. Processing the 4000 m Aperture

A full water column aperture array is now assumed deployed instead of the 1000 m array. This array has 323 sensors with 12.353 m interelement spacing. Initial beamforming results with the large aperture array do not yield dramatic differences whether or not the source is on the shelf slope or beyond, that is whether or not there is downslope conversion. To resolve the structure of the MFP ambiguity surface better, several plots of ambiguity surfaces with different normalizations and dynamic ranges are presented.

The ambiguity surfaces of the four different stations, given by Eq. (2), are gray-level displayed in Figs. 23 to 26 with a 20 dB dynamic range. The two stations where strong

slope conversion takes place (i.e. when the source is in shallow water or above the small slope), have ambiguity surfaces with fairly broad peaks. These peaks are distributed in depth mostly around 200 m, 500-600 m and 800-900m. As usual, convergence zone periodicity in range is observed. When the sources above the steep slope and at the beginning of the gentle slope, there is minimal downslope conversion, and the corresponding MFP ambiguity surfaces have much greater granularity. They appear to have a higher spatial frequency content with finer structure in both range and depth. Many small peaks are distributed in range with a convergence zone periodicity which is more pronounced than in the case of the slope interacting stations. Also, the highest correlation levels appear to be towards the surface rather than larger depths. These observations are confirmed by the plots of the ambiguity surfaces normalized by their highest peak and gray-level displayed on a 10 dB scale, in Figs. 27 to 30.

As in Section 4.1, it is of interest to look at the ambiguity surfaces due to a shallow (45 m) and a deep (305 m) source within the MFP search window, 423 km away from the receiving array. The ambiguity surface due to the shallow source is gray-level displayed in Fig. 31. It is formed of inverted V shaped patterns with a convergence periodicity in range. Closer to the array, the well delimited patterns are destroyed and tend to form blocks of fine peaks peaks distributed in depth and range. As in the case of the 1000 m aperture, the ambiguity surface due to the shallow source in the MFP search window and the ambiguity surfaces of the non slope interacting stations have an overall fine structure in common. The ambiguity surface when the source is at 305 m depth is gray-level displayed in Fig. 32. The ambiguity surface has the familiar butterfly pattern centered at the source location. These patterns change shape with range and tend to spread at closer ranges to the array. This character is similar to the one observed for the slope interacting stations (see Figs. 29 and 30).

Reducing the dynamic range of the gray-level plot from 20 down to 10 dB has a

clipping effect and removes most of the lower correlation level structure in the surface given by Eq.(1). These ambiguity surfaces given in Figs. 33 to 36 give an opportunity of detecting the main structural changes in the ambiguity fields when the source does or does not interact with the slope. Indeed, one can observe in the case of the source in shallow water and above the small slope, peaks distributed in depth around 200 m as well as deeper, below 500 m. These deep ambiguity peaks are not observed in the ambiguity surfaces of the sources above the steep slope and at the beginning of the gentle slope sector. In those surfaces, only a few peaks around 100 m are observed. It is of interest to compare these surfaces with the ones (with the same normalization) corresponding to a source within the range-depth MFP window, at 423 km range at two different depths : 45 m or 305 m depth. The ambiguity surfaces are given in Figs. 37 and 38. There is a strong similarity between the ambiguity surface of the source at 45 m depth and 423 km range and the one of the non-slope interacting stations. There is as well a strong similarity between the ambiguity surface of the source at 305 m depth and 423 km range and the one of the slope interacting stations.

Table 2 provides quantitative results of matched-field processing on the full water column array. The correlation values for this 323 sensor array are still high, around 0.3. The depth of the highest peak does not correlate as clearly with the slope interaction, as in the case of the 1000 m aperture. This is consistent with the fact that the ambiguity surfaces are not dramatically different whether or not there is downslope conversion as they are for the 1000 m aperture.

5. Conclusions

The manifestation of sources on the continental slope in the deep water MFP ambiguity surface has been studied in this report. The PE model is used to simulate the pressure fields due to a low frequency (18 Hz) shallow source that has propagated over 1750 km. Two receiving arrays are considered: (1) a 1000 m aperture with 80 sensors deployed

from 400 to 1390 m and (2) a full water column array with 323 sensors. In both cases, the interelement spacing is constant and equal to 12.353 m. The environment is range dependent in both bathymetry and sound speed. After a preliminary analysis of the simulated pressure fields was carried out using transmission loss plots, field plots and conventional plane-wave beamforming, matched-field ambiguity surfaces were calculated on a range-depth search window extending in range from 25 to 525 km and in depth from 5 to 985 m. These surfaces were studied when the source was (1) on the continental shelf in shallow water, 1750 km from the receiving array, (2) above a small 2.8 deg. slope, (3) above a steep 11.5 deg. slope, and finally (4) in deep water at the beginning of a gentle 0.4 deg. slope sector where the deep water begins.

Array design has an impact on the appearance of the MFP ambiguity surfaces. The shorter array (1000 m) deployed across the sound axis yields very different results whether or not the source is at a location where downslope conversion takes place. When the source is above the small slope sector and in shallow water, the MFP ambiguity surfaces have broad peaks at large depths. The shallow source looks like a deep source because of downslope conversion. On the other hand, when the source is above the steep slope or at the beginning of the gentle slope, there is no slope interaction and the ambiguity surfaces have smaller peaks at shallow depth. The shallow source still looks like a shallow source. For this array configuration, both conventional beamforming and matched-field processing results show that shoaling of the sound axis towards the continental slope (which is another proposed mechanism for the coupling of sound in the deep sound channel [5,8]) has little impact.

The results obtained with the 4000 m array (full water column aperture) are not as dramatic as the shorter array results, although a careful analysis of the MFP ambiguity surfaces lead to the observation of definite differences between the slope interacting and non-interacting sources. The character of the MFP ambiguity surfaces for sources which do

not interact with the slope and of a shallow source in deep water are similar. They have a fine structure and a concentration of the strongest peaks towards the surface. On the other hand, the ambiguity surfaces of the slope interacting sources have larger features distributed at larger depths. These latter are similar to the ambiguity surfaces of deep sources in deep water.

For both array apertures, high MFP correlation values (Eq. (1)) are observed with values between 0.6 and 0.7 for the 1000 m array and between 0.23 and 0.32 for the full water column array. This means that an 18 Hz source on the continental shelf and at large range can look like a source in deep water at closer range to the array. The highest correlation values are observed when the shallow source is above the small 2.8 deg. slope where there is maximum slope interaction.

6. Acknowledgments

This work was supported by the Office of Naval Research under contract # N00014-91-J-1237. Thanks are due to the authors of the PE model and of the KRAKEN normal mode model.

7. References

[1] W. Hodgkiss, "Downslope conversion", NATO Advanced Study Institute on Acoustic Signal Processing for Ocean Exploration, 27 Jul.-7 Aug. 1992, Madeira, Portugal.

[2] S. E. Dosso and N. R. Chapman, "Measurement and modeling of downslope acoustic propagation loss over a continental shelf", J. Acoust. Soc. Am., 81(2), Feb. 1987, pp. 258-268.

[3] W. M. Carey, "Measurement of downslope sound propagation from a shallow source to a deep receiver", J. Acoust. Soc. Am., 79(1), Jan. 1986, pp. 49-59.

[4] W. M. Carey, I. B. Gereben and B. A. Brenson, "Measurement of sound propagation downslope to a bottom limited sound channel", J. Acoust. Soc. Am., 81(2), Feb. 1987, pp. 244-257.

[5] R. A. Wagstaff, "Low frequency ambient noise in the deep sound channel, the missing component", J. Acoust. Soc. Am., 69(4), April 1981, pp. 1009-1014.

[6] S. C. Wales and O. I. Diachok, "Ambient noise vertical directionality in the northwest Atlantic", J. Acoust. Soc. Am., 70(2), Aug. 81, pp. 577-582.

[7] N. R. Chapman, J. M. Syck and G. R. Carlow, "Vertical directionality of acoustic signals propagating downslope to a deep ocean receiver", in *Progress in Underwater Acoustics*, H. M. Merklinger, Ed., Plenum Press, 1987, pp. 573-579.

[8] W. C. Carey, R. B. Evans, J. A. Davis and G. Botseas, "Deep ocean vertical noise directionality", IEEE J. Oceanic Eng., Vol 15, No 4, Oct. 1990, pp. 324-334.

[9] F. B. Jensen and M. G. Martinelli, The SACLANTCEN parabolic equation model (PAREQ), SACLANT ASW Res. Ctr., La Spezia, Italy, 1985.

[10] F. D. Tappert, "The parabolic approximation method", in *Wave propagation and underwater acoustics*, J. B. Keller and J. S. Papadakis, Eds., Berlin: Springer-Verlag, 1977, pp. 224-281.

[11] D. J. Thomson and N. R. Chapman, "A wide angle split-step algorithm for the parabolic equation", J. Acoust. Soc. Am., 74(6), Dec. 1983, pp. 1848-1854.

[12] M. Olivera, Downslope conversion experiment : Environmental data report, Marine Physical Laboratory Technical Memorandum 414, MPL-U-1/90, Scripps Institution of Oceanography, Jan. 1990.

[13] M. Porter, The KRAKEN normal mode model, SACLANT ASW Res. Ctr., SACLANTCEN Memorandum, SM-245, Sept. 1991.

[14] J-M. Tran, Approaches to the processing of data from large aperture vertical line arrays, Ph.D. Dissertation, Univ. California, San Diego, SIO Ref. 90-21, April 1990.

Table 1. Quantitative results of matched-field processing on the 1000 m array.

Station	Correlation	Depth (m)	Range (km)
Shallow water	0.64303	565	513
Small Slope	0.69464	725	525
Steep Slope	0.66555	105	351
Gentle Slope	0.65828	105	203

Table 2. Quantitative results of matched-field processing on the 4000 m array.

Station	Correlation	Depth (m)	Range (km)
Shallow water	0.64303	565	513
Small Slope	0.69464	725	525
Steep Slope	0.66555	105	351
Gentle Slope	0.65828	105	203

List of Figures

Fig. 27 : Normalized MFP ambiguity surface for the 45 m deep source located on the continental shelf, 1750 km from the 4000 m long array.

Fig. 28 : Normalized MFP ambiguity surface for the 45 m deep source located on the small 2.8 deg. slope, 1729.6 km from the 4000 m long array.

Fig. 29 : Normalized MFP ambiguity surface for the 45 m deep source located on the steep 11.5 deg. slope, 1711.9 km from the 4000 m long array.

Fig. 30 : Normalized MFP ambiguity surface for the 45 m deep source located at the beginning of the gentle 0.4 deg. slope, 1707.5 km from the 4000 m long array.

Fig. 31 : MFP ambiguity surface for the 45 m deep source located 423 km from the 4000 m long array.

Fig. 32 : MFP ambiguity surface for the 305 m deep source located 423 km from the 4000 m long array.

Fig. 33 : MFP ambiguity surface for the 45 m deep source located on the continental shelf, 1750 km from the 4000 m long array. The dynamic range is reduced to 10 dB.

Fig. 34 : MFP ambiguity surface for the 45 m deep source located on the small 2.8 deg. slope, 1729.6 km from the 4000 m array. The dynamic range is reduced to 10 dB.

Fig. 35 : MFP ambiguity surface for the 45 m deep source located on the the steep 11.5 deg. slope, 1711.9 km from the 4000 m long array. The dynamic range is reduced to 10 dB.

Fig. 36 : MFP ambiguity surface for the 45 m deep source located at the beginning of the gentle 0.4 deg. slope, 1707.5 km from the 4000 m long array. The dynamic range is reduced to 10 dB.

Fig. 37 : MFP ambiguity surface for the 45 m deep source located 423 km from the 4000 m long array. The dynamic range is reduced to 10 dB.

Fig. 38 : MFP ambiguity surface for the 305 m deep source located 423 km from the 4000 m long array. The dynamic range is reduced to 10 dB.

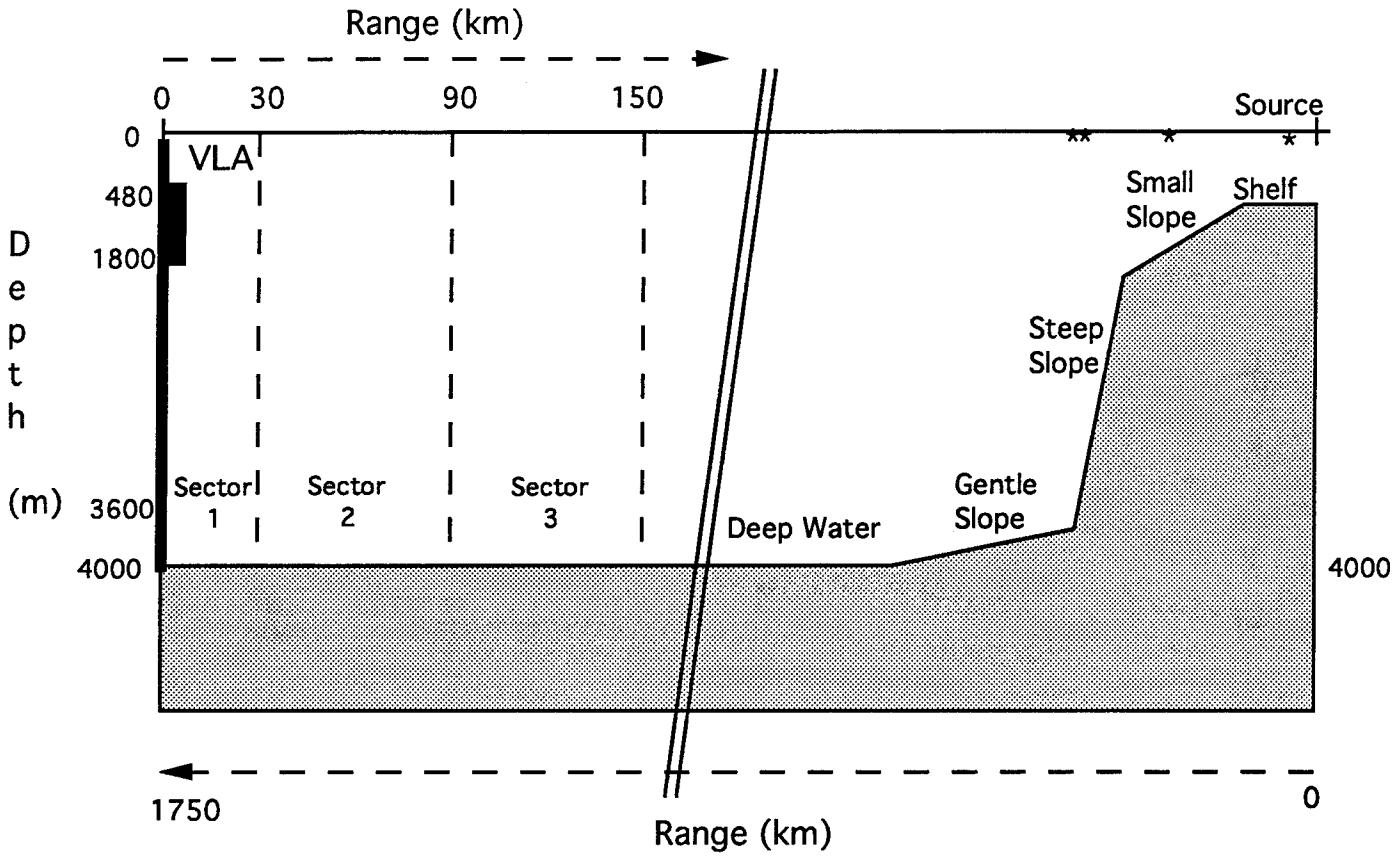
Range (km)
0
30
90
150
Source
VLA
0
480
1800
3600
4000
Depth (m)
Sector 1
Sector 2
Sector 3
Deep Water
Gentle Slope
Steep Slope
Small Slope
Shelf
4000
1750
0
Range (km)

Figure 2

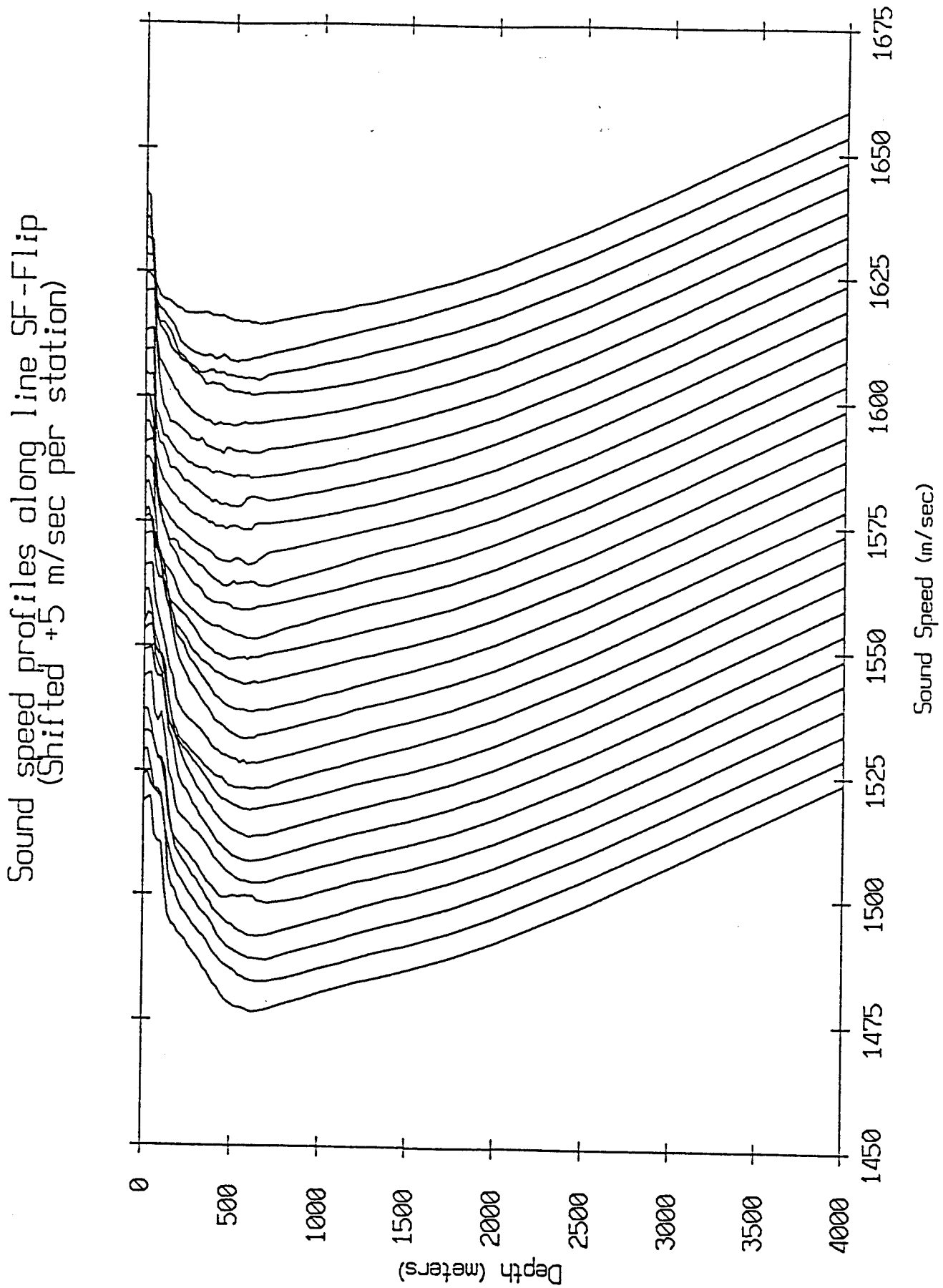
Sound speed profiles along line SF-Flip
(Shifted +5 m/sec per station)
Depth (meters)
0
500
1000
1500
2000
2500
3000
3500
4000
1450
1475
1500
1525
1550
1575
1600
1625
1650
1675
Sound Speed (m/sec)

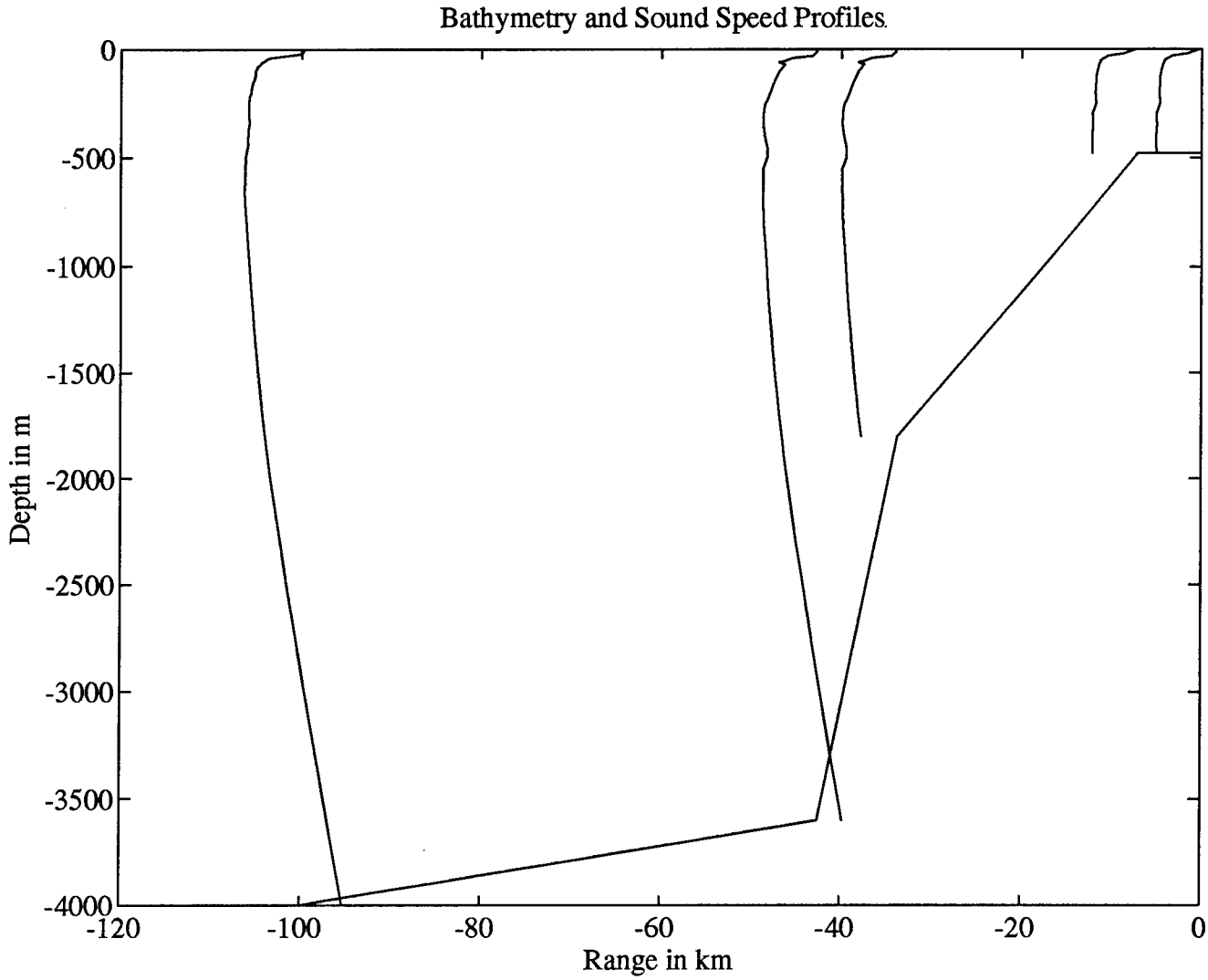
Bathymetry and Sound Speed Profiles
0
-500
-1000
-1500
-2000
-2500
-3000
-3500
-4000
Depth in m
-120
-100
-80
-60
-40
-20
0
Range in km

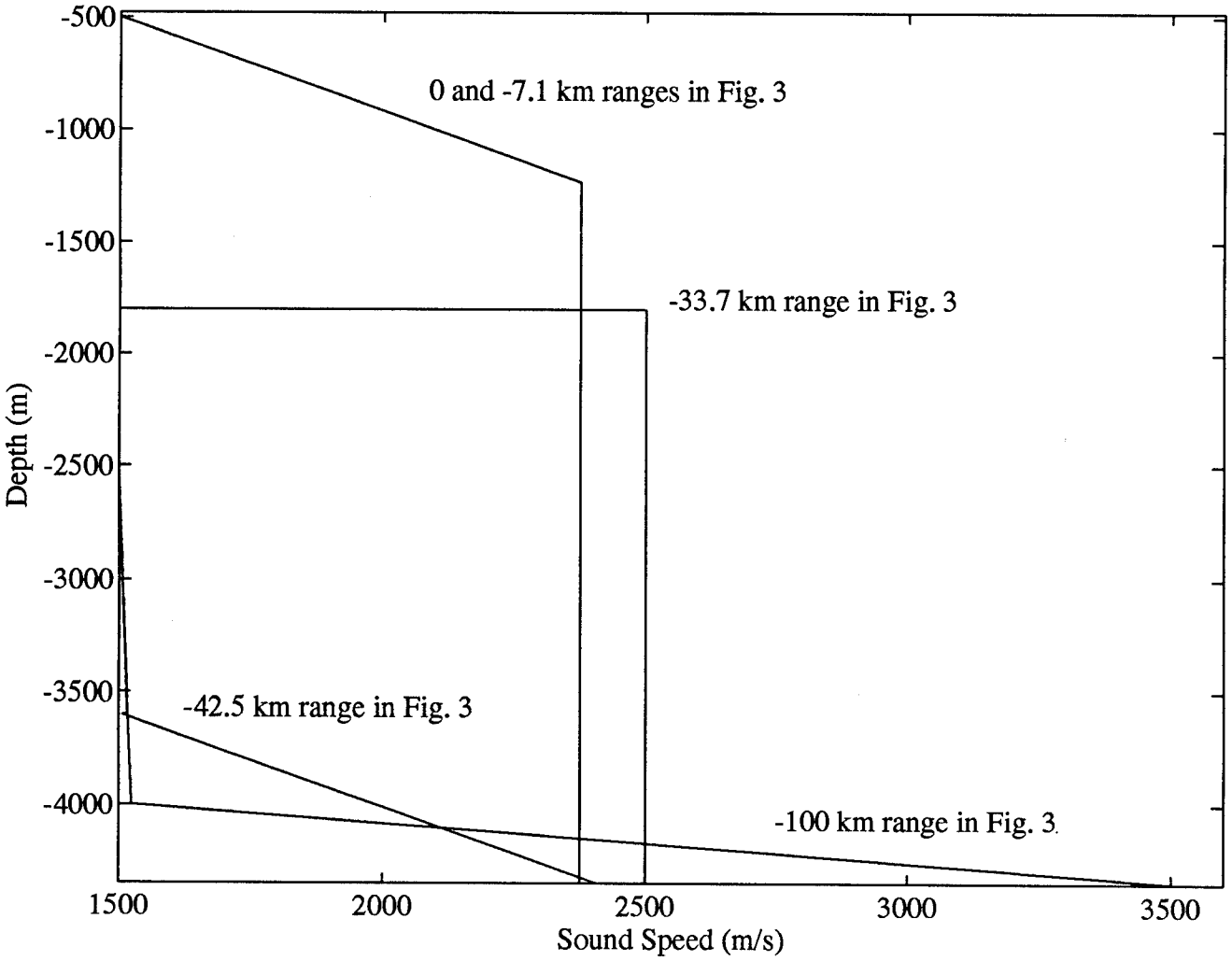
-500
-1000
-1500
-2000
-2500
-3000
-3500
-4000
Depth (m)
0 and -7.1 km ranges in Fig. 3
-33.7 km range in Fig. 3
-42.5 km range in Fig. 3
-100 km range in Fig. 3
1500
2000
2500
3000
3500
Sound Speed (m/s)

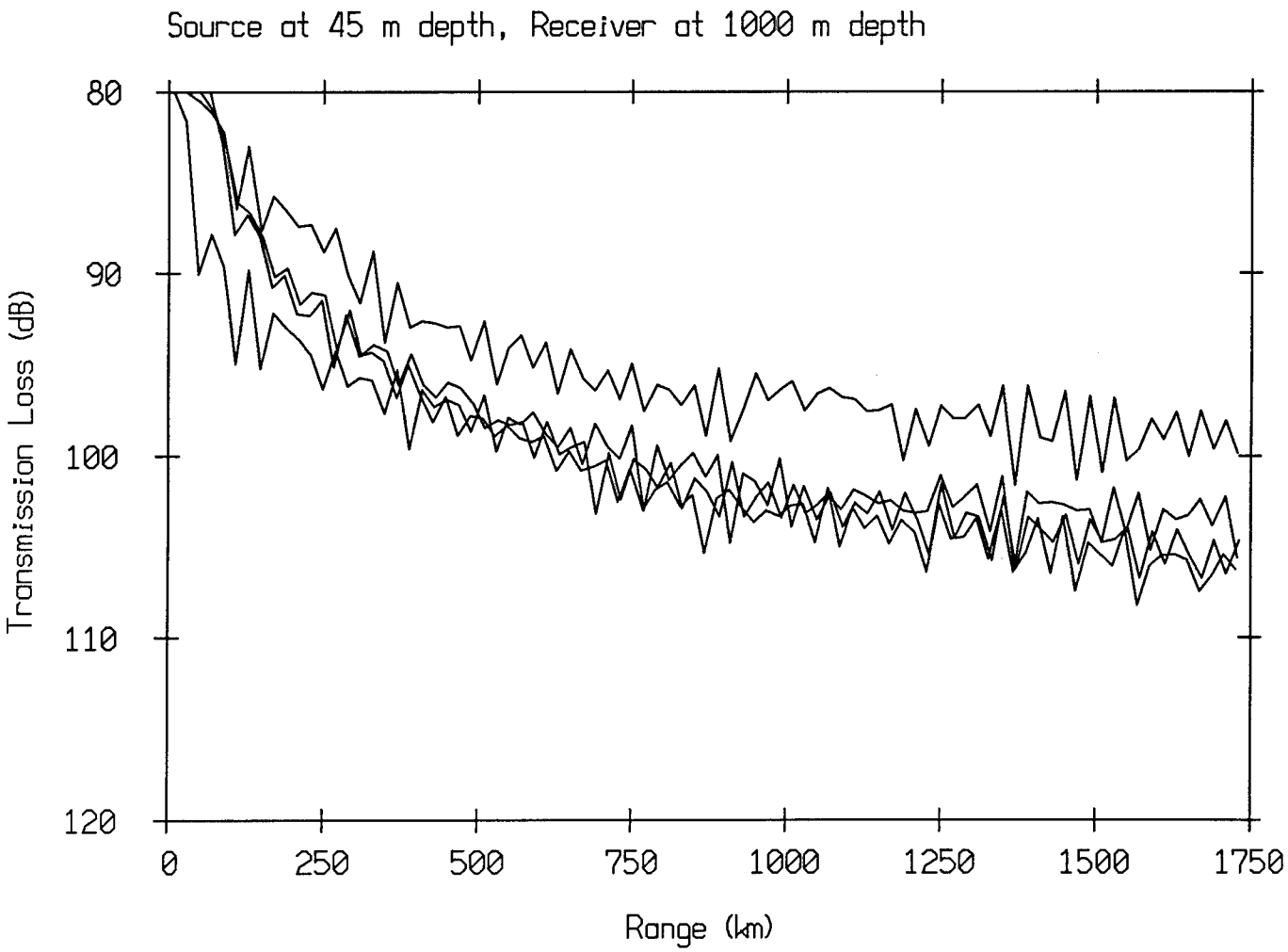
Source at 45 m depth, Receiver at 1000 m depth
Transmission Loss (dB)
80
90
100
110
120
0
250
500
750
1000
1250
1500
1750
Range (km)

Transmission Loss
Source (45 m deep) out of the MFP window
in shallow water

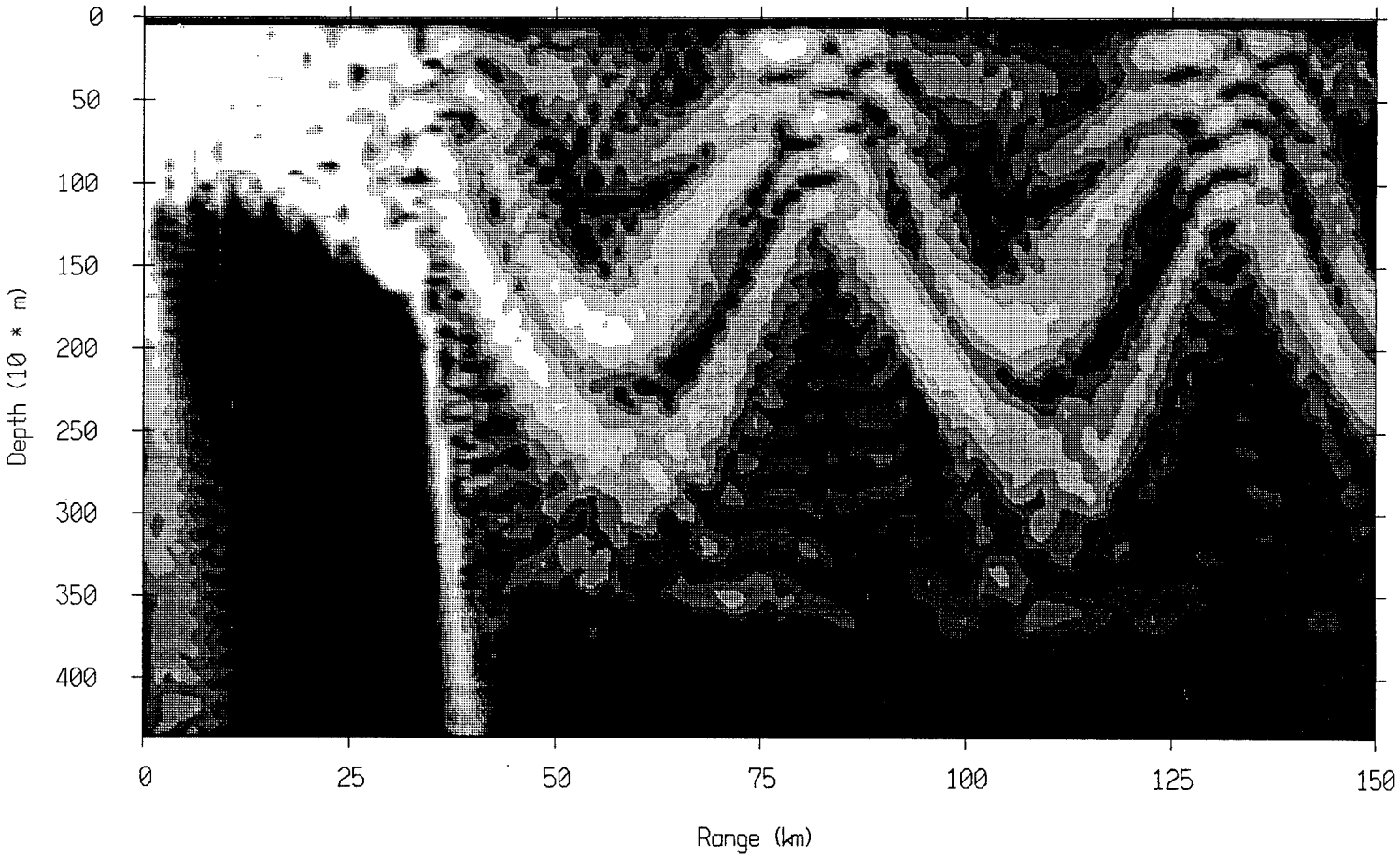

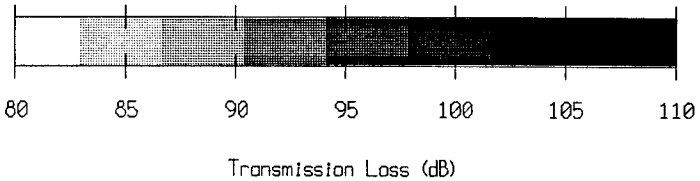

Bathymetry : Source in shallow water

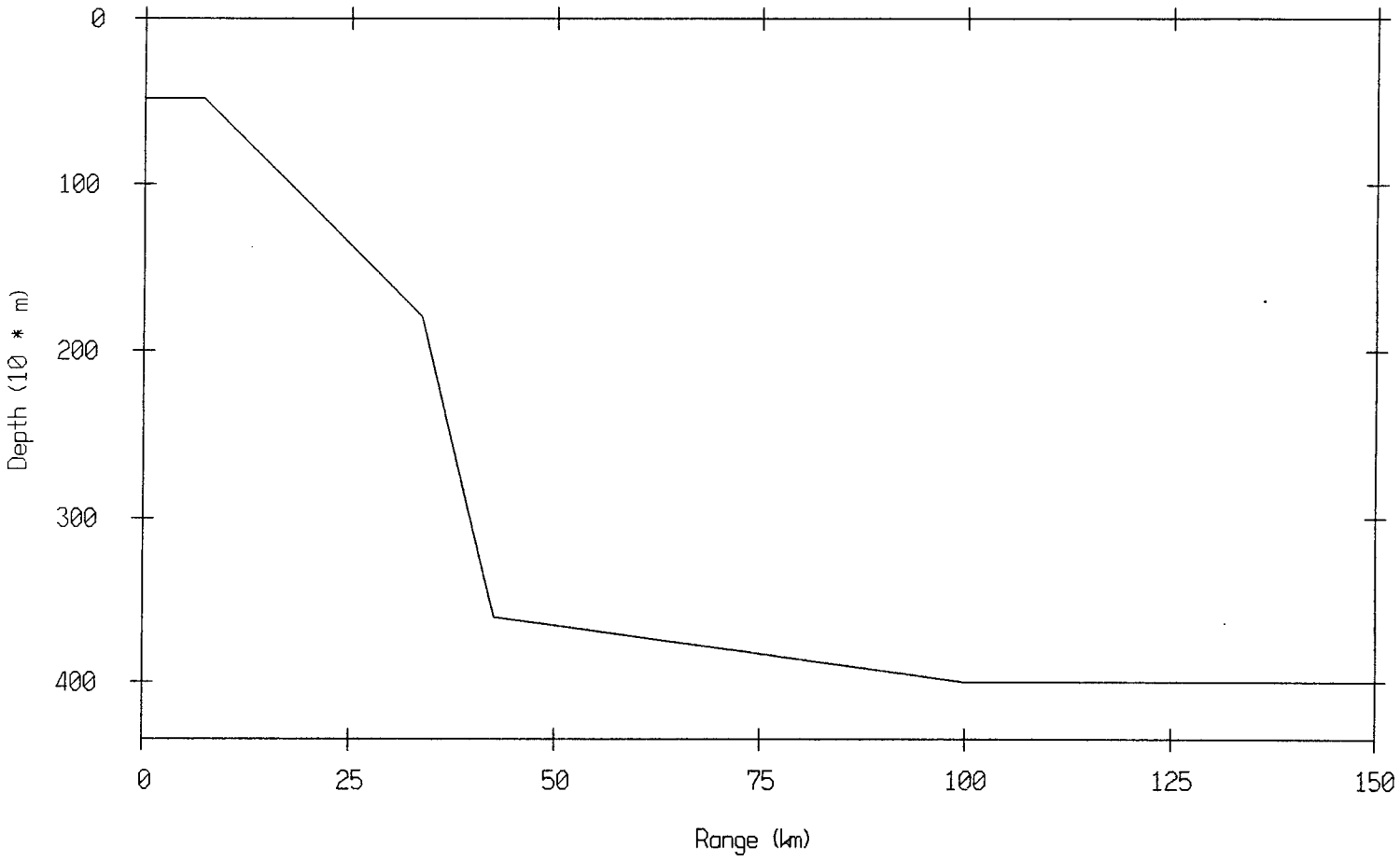

Transmission Loss
Source (45 m deep) out of the MFP window
in small slope sector

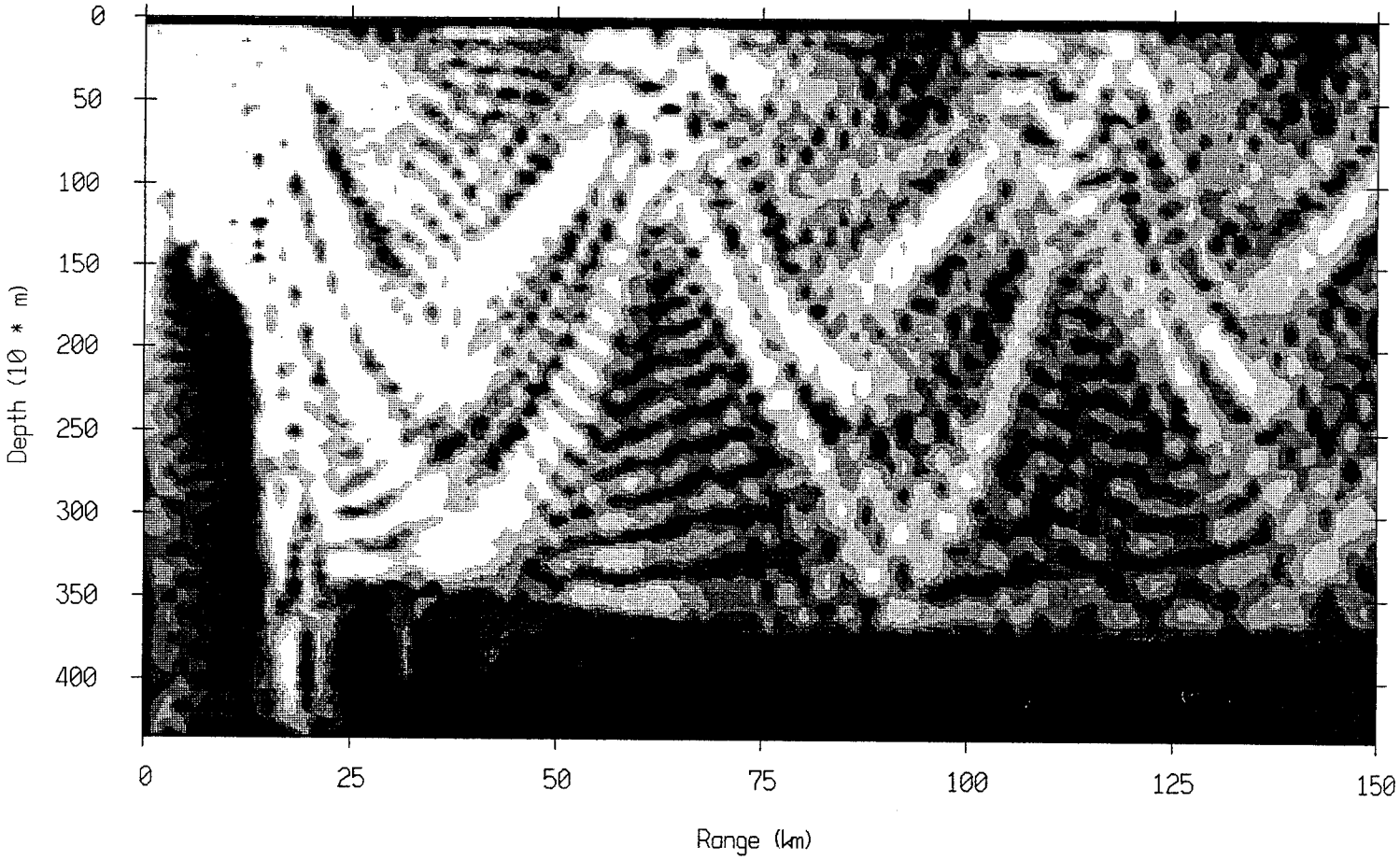

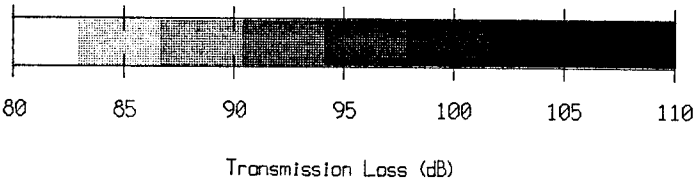

Bathymetry : Source in small slope sector

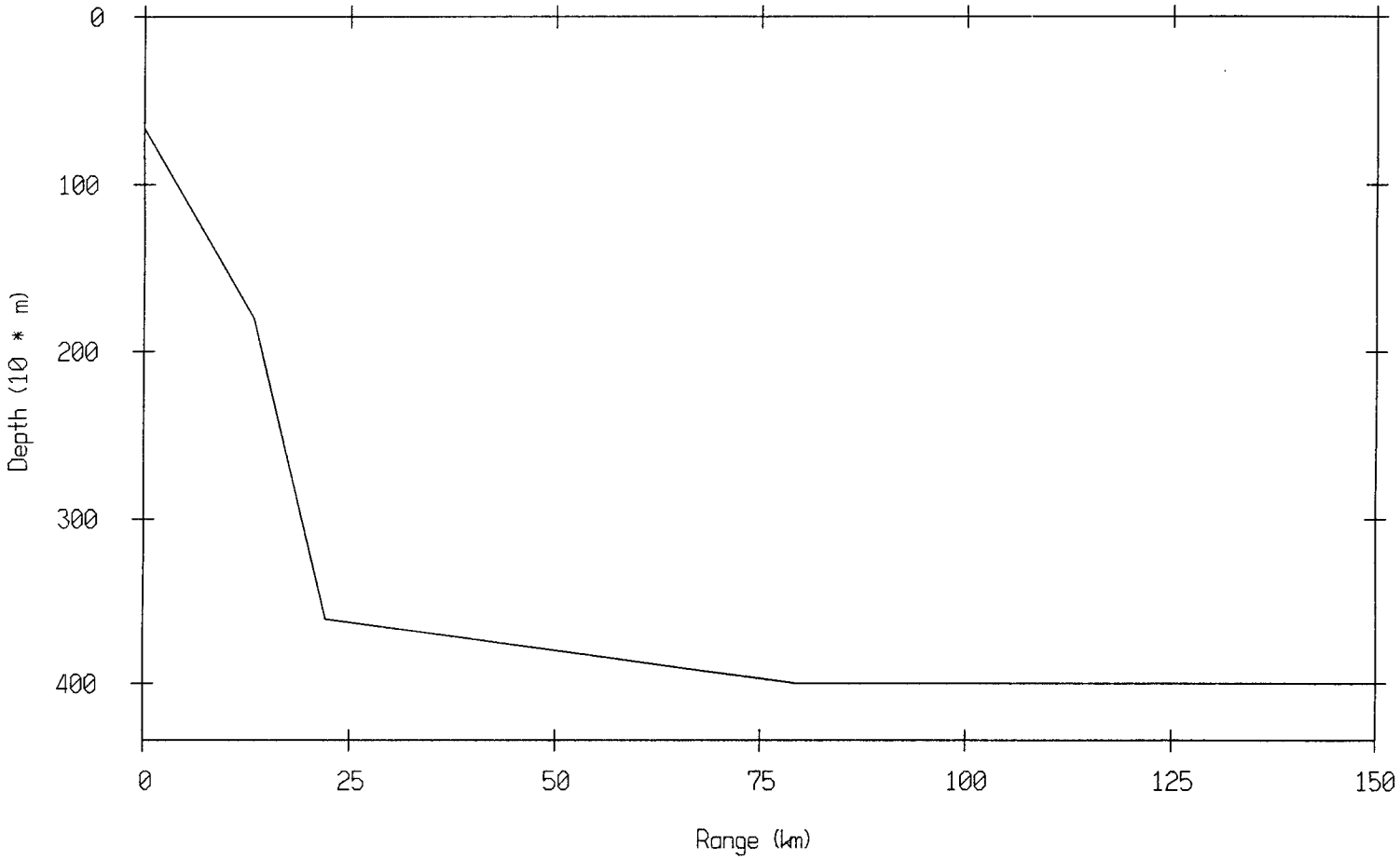

Transmission Loss
Source (45 m deep) out of the MFP window
in steep slope sector

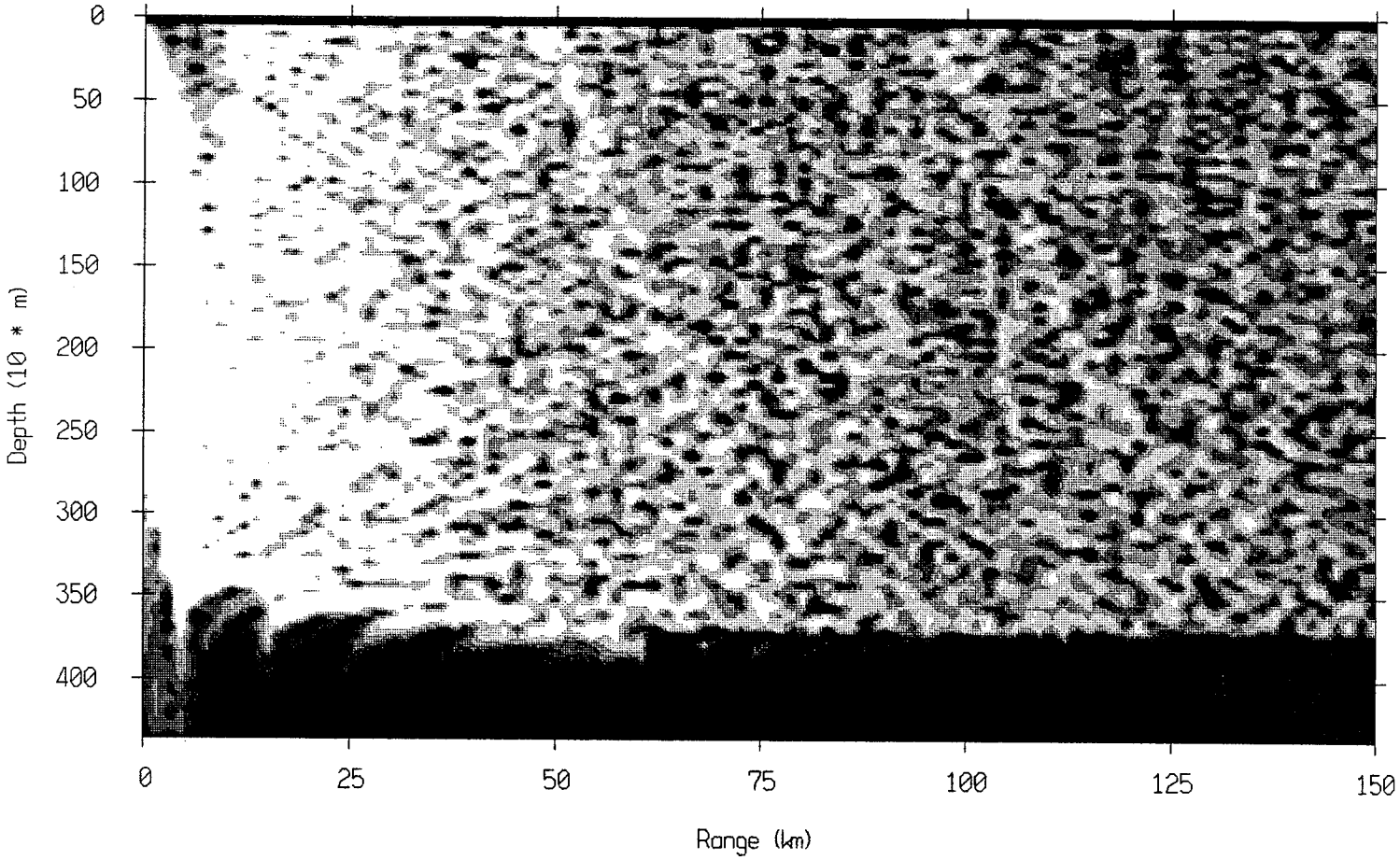

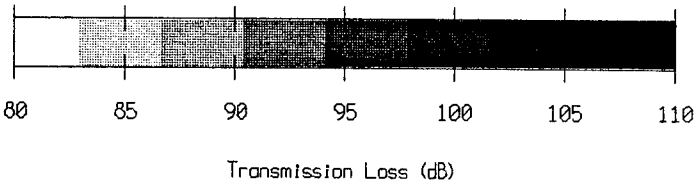

Bathymetry : Source in steep slope sector

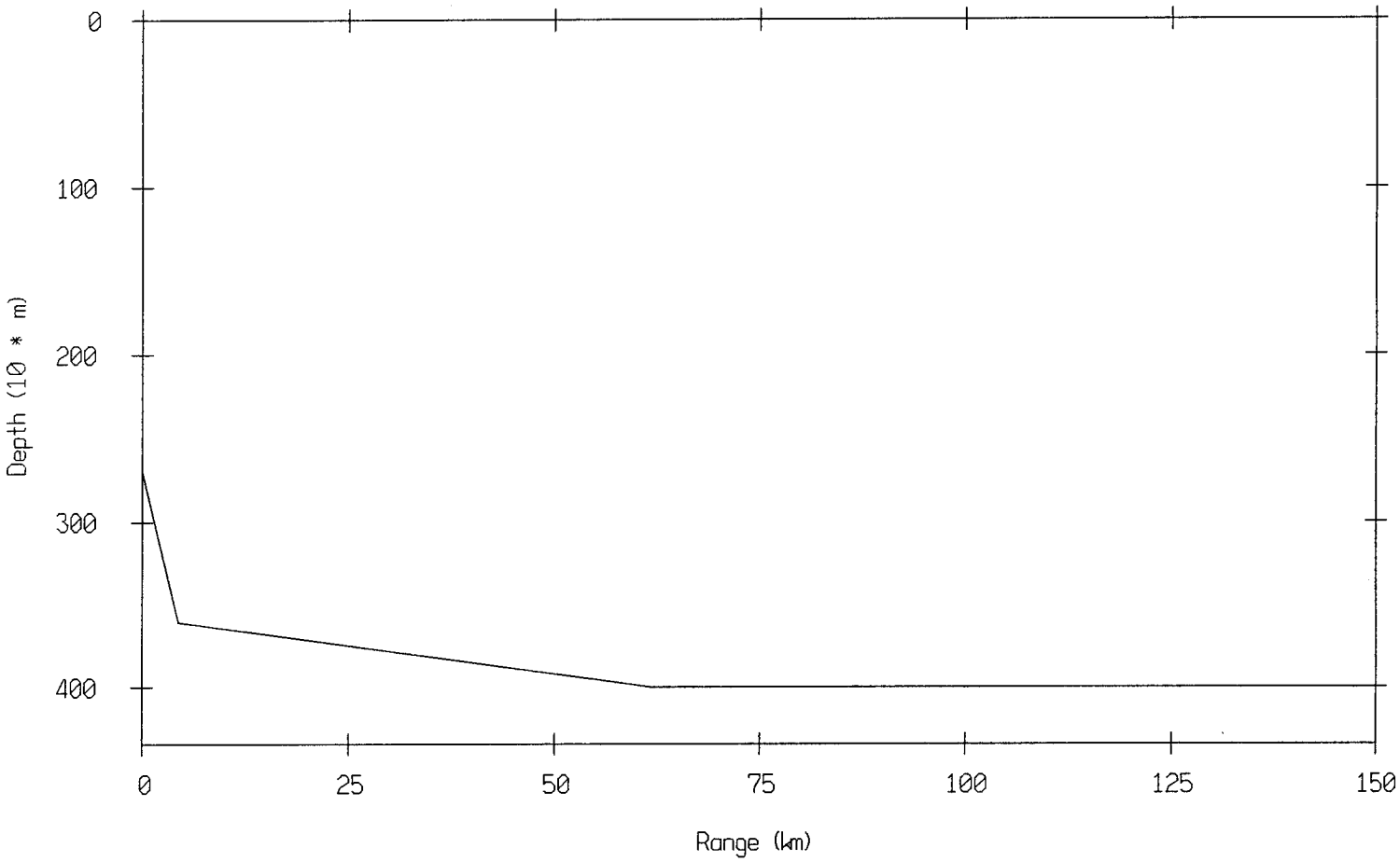

Transmission Loss
Source (45 m deep) out of the MFP window
in gentle slope sector

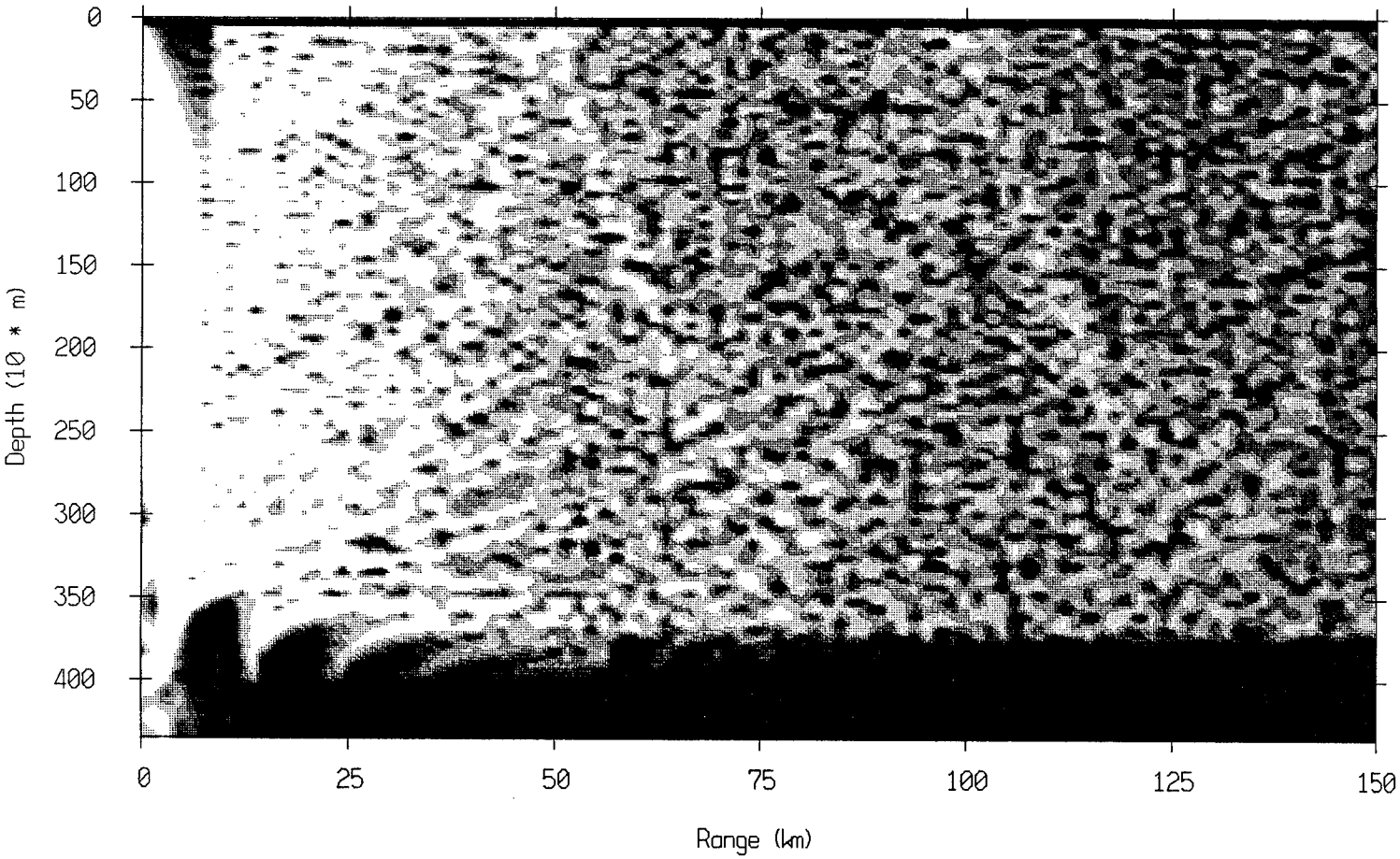

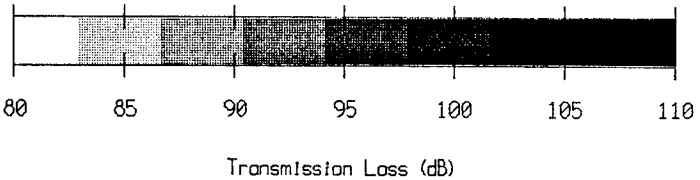

Bathymetry : Source in gentle slope sector

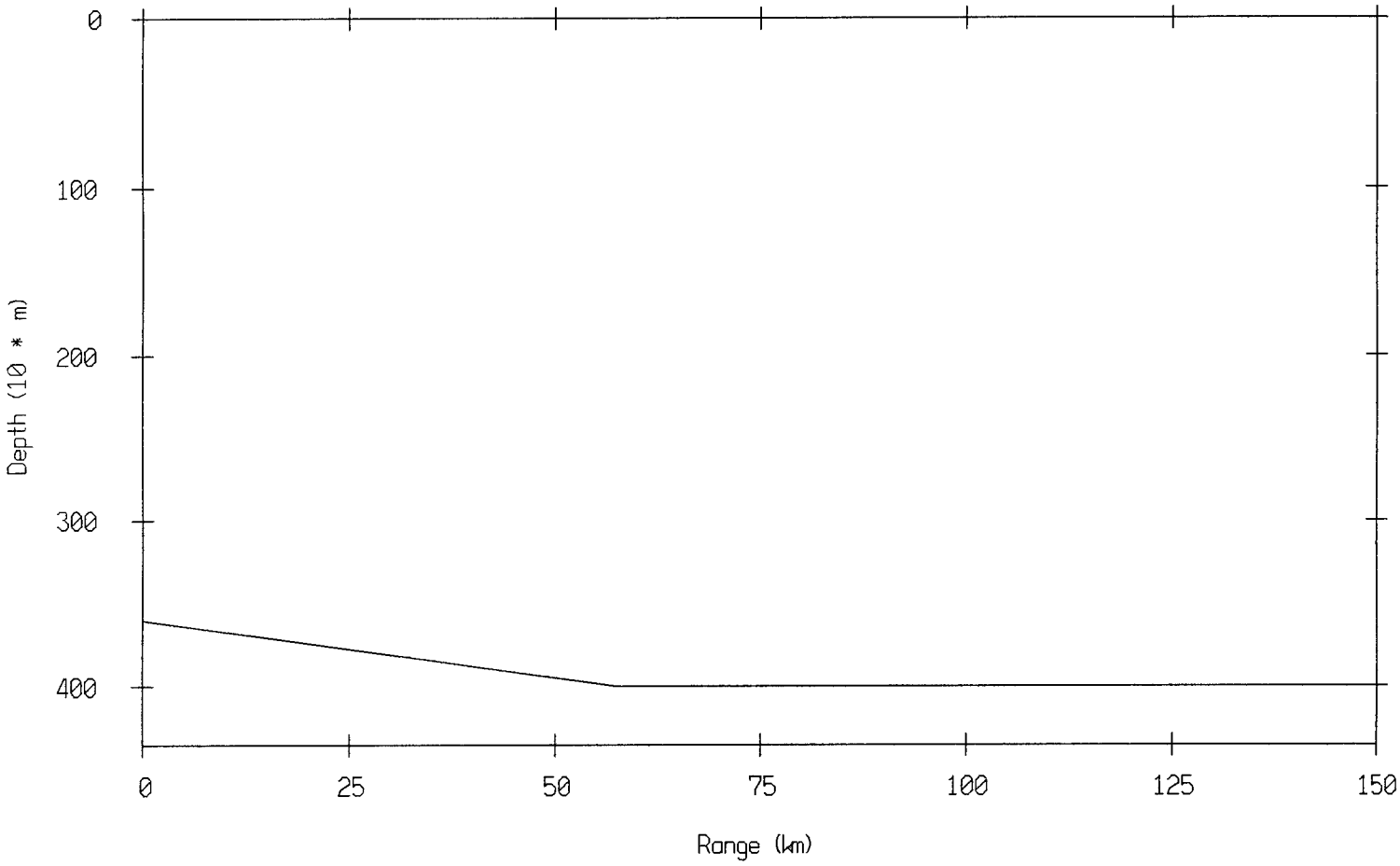

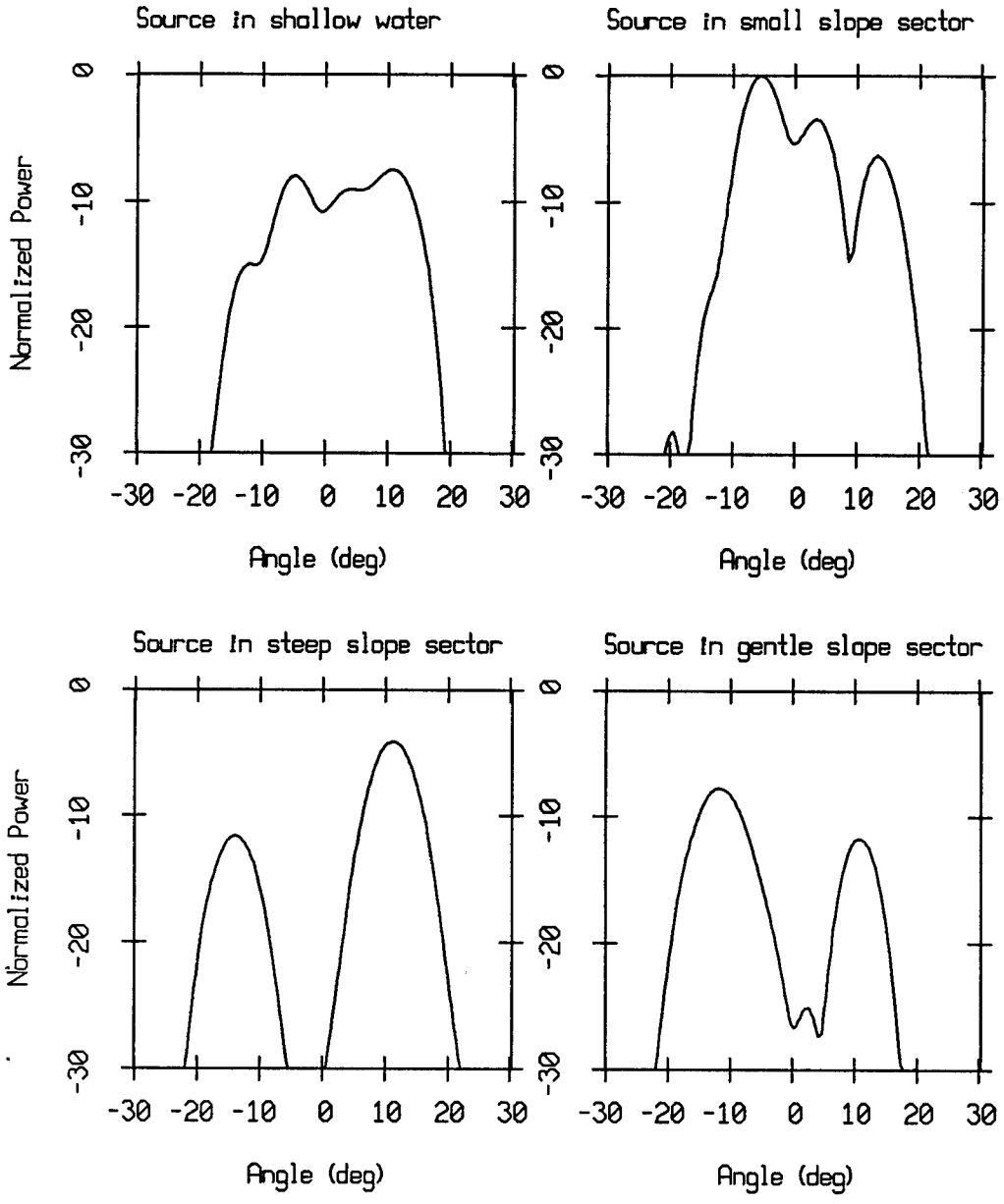
Source in shallow water
Source in small slope sector
Source in steep slope sector
Source in gentle slope sector
Normalized Power
0
-10
-20
-30
-30 -20 -10 0 10 20 30
Angle (deg)

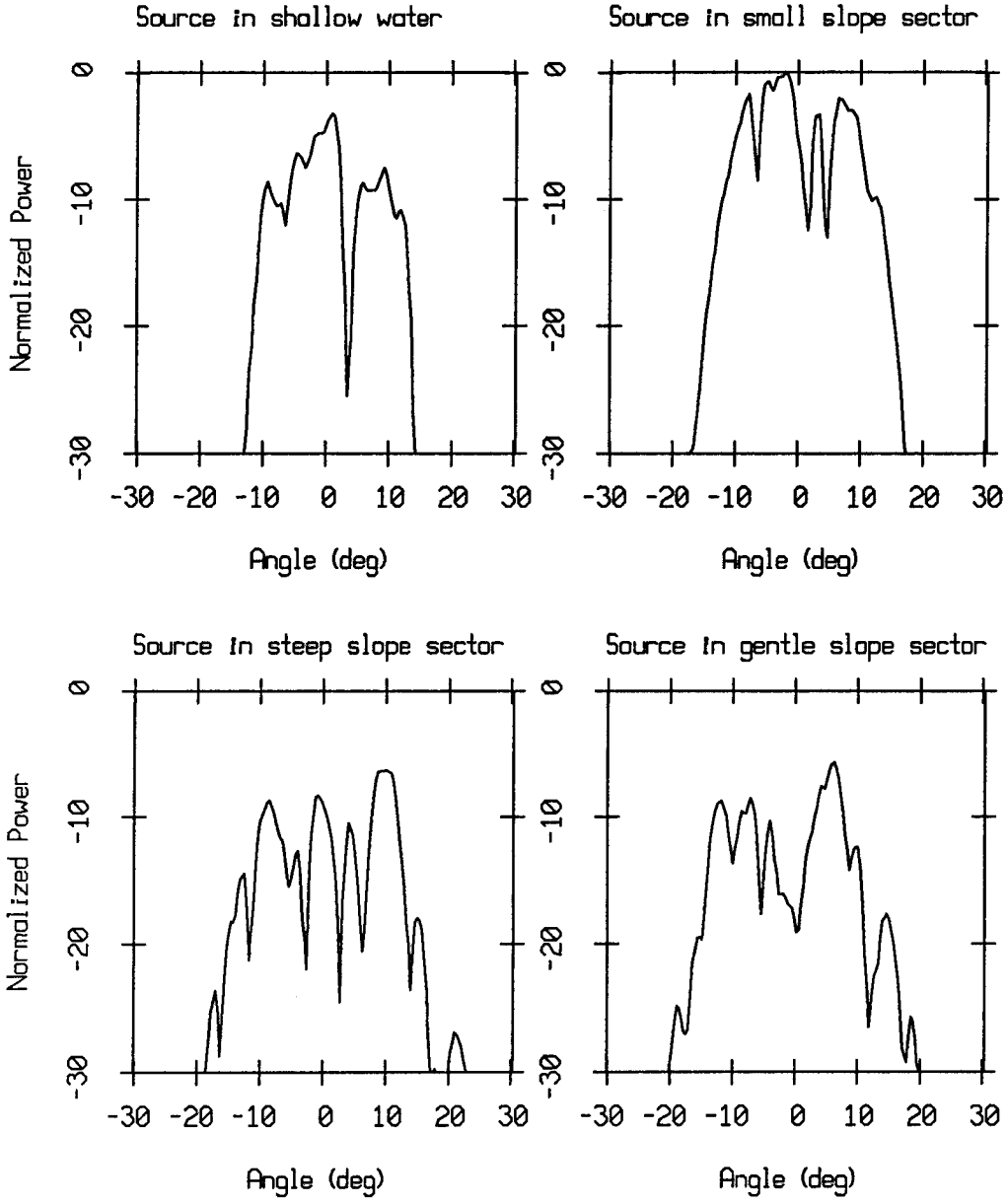
Source in shallow water
Source in small slope sector
Source in steep slope sector
Source in gentle slope sector
Normalized Power
0
-10
-20
-30
-30 -20 -10 0 10 20 30
Angle (deg)

Source out of the MFP window at 45 m depth
1000 m array with 12.353 m interelement spacing
Shallow water sector

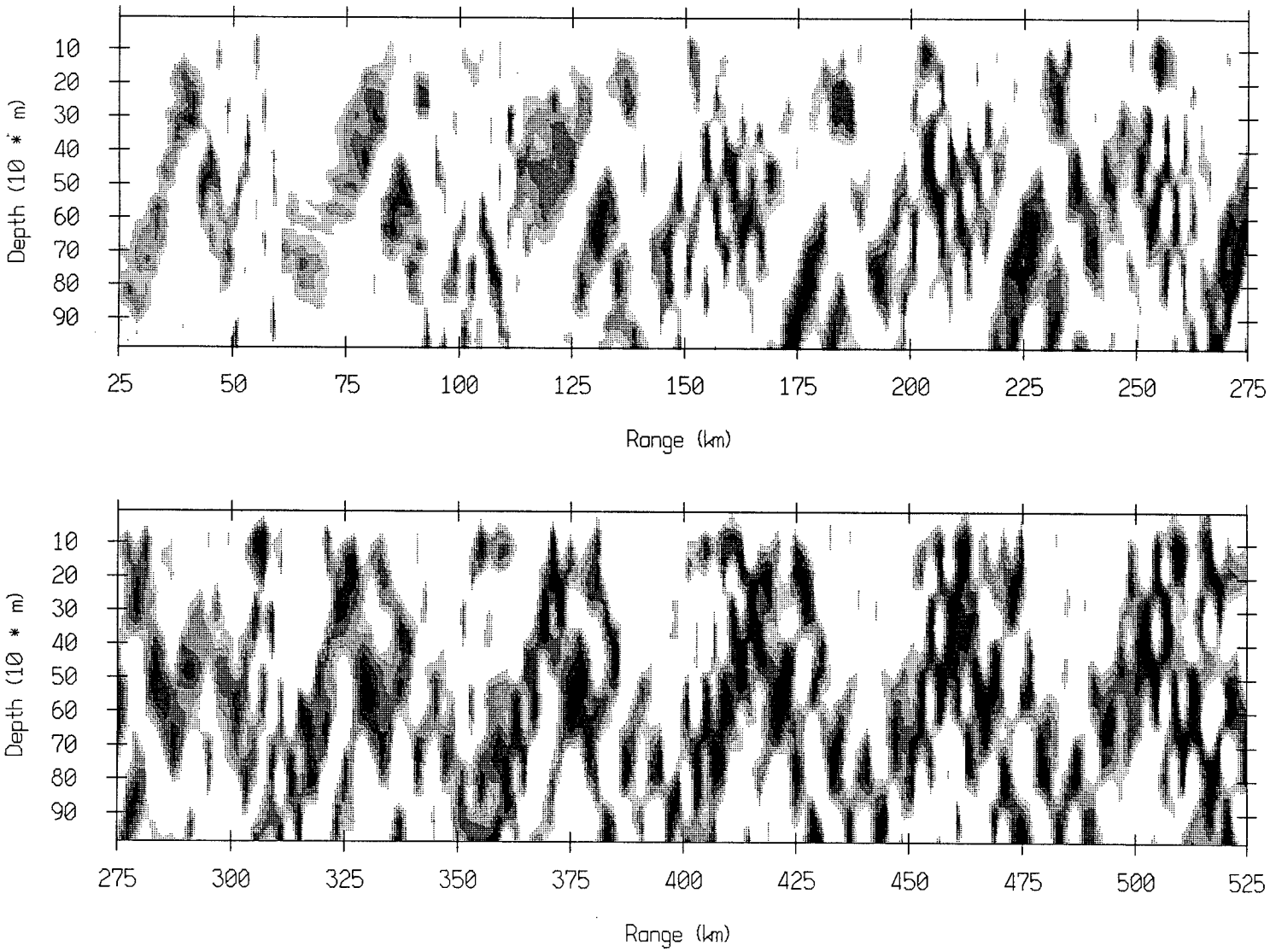

Source out of the MFP window at 45 m depth
1000 m array with 12.353 m interelement spacing
Small slope sector

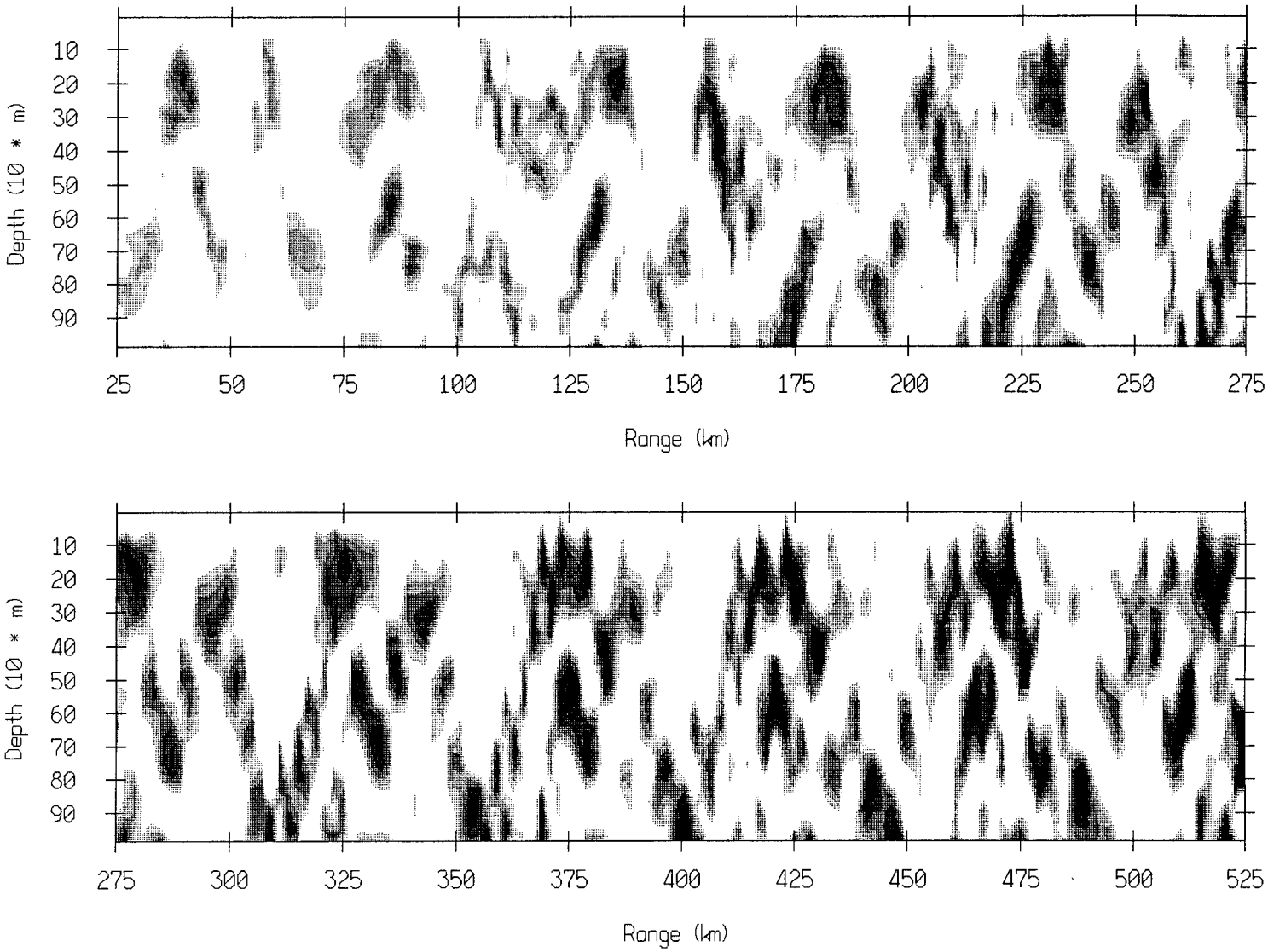

Source out of the MFP window at 45 m depth
1000 m array with 12.353 m interelement spacing
Steep slope sector

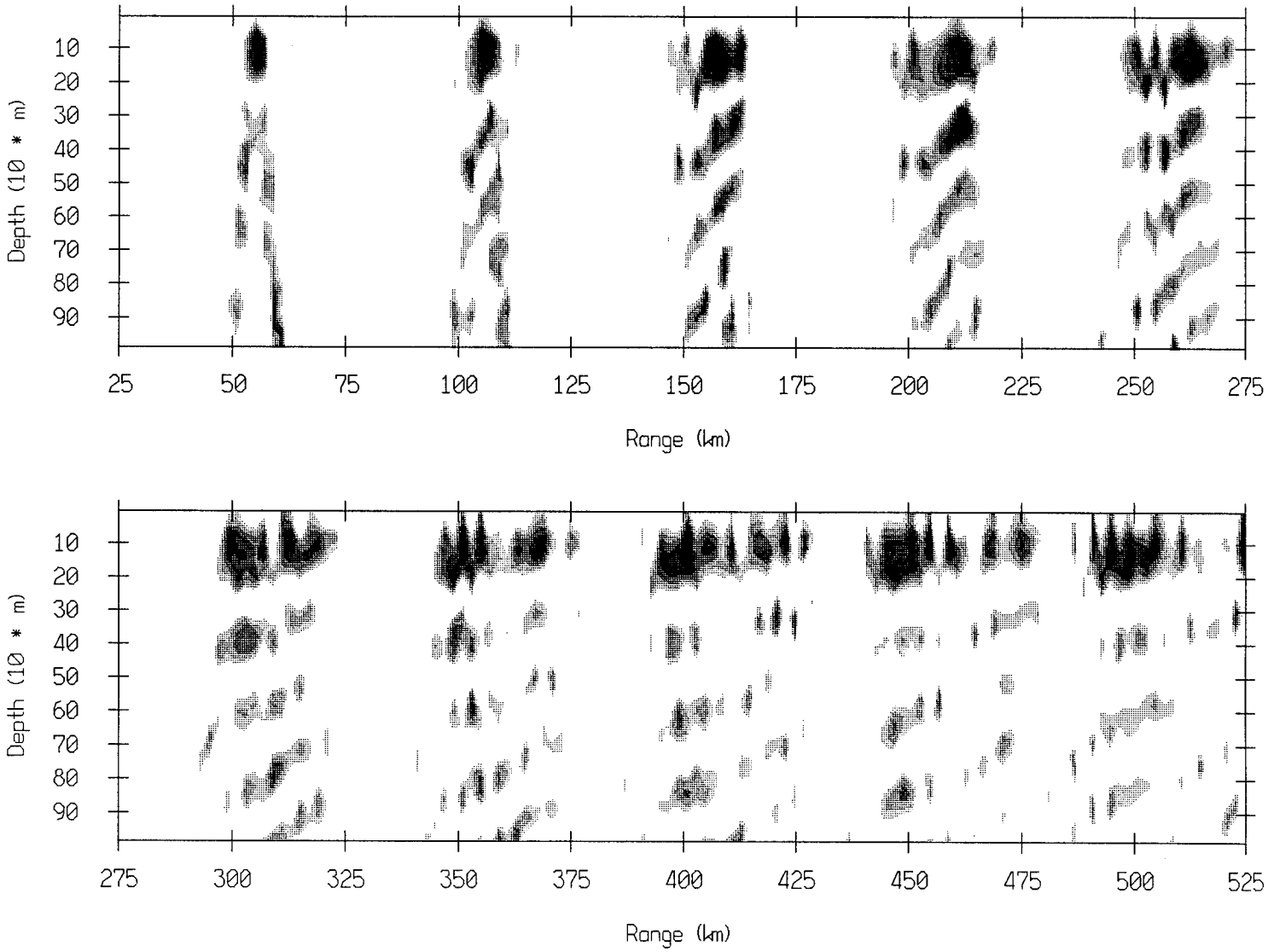

Source out of the MFP window at 45 m depth
1000 m array with 12.353 m interelement spacing
Gentle slope sector

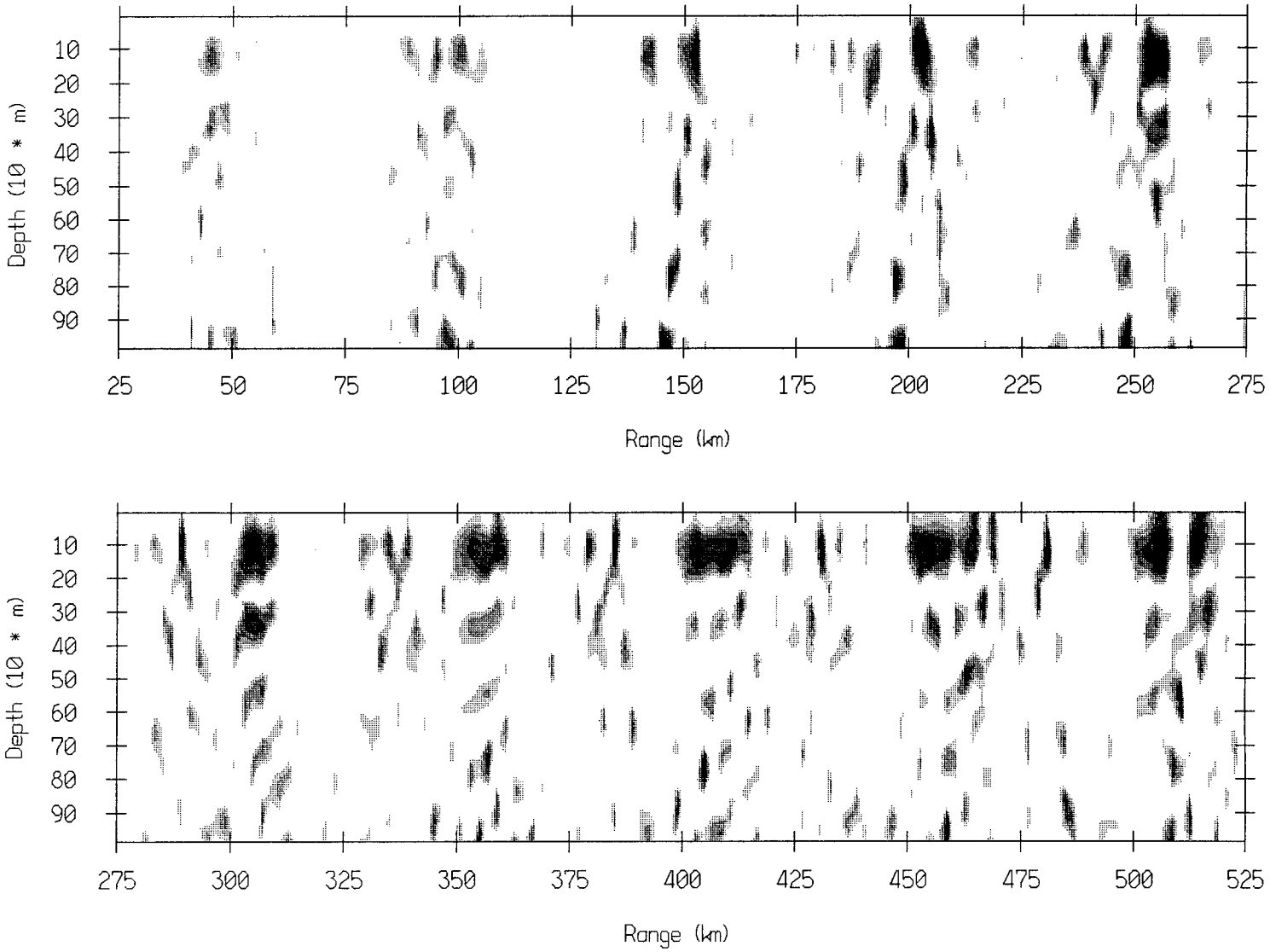

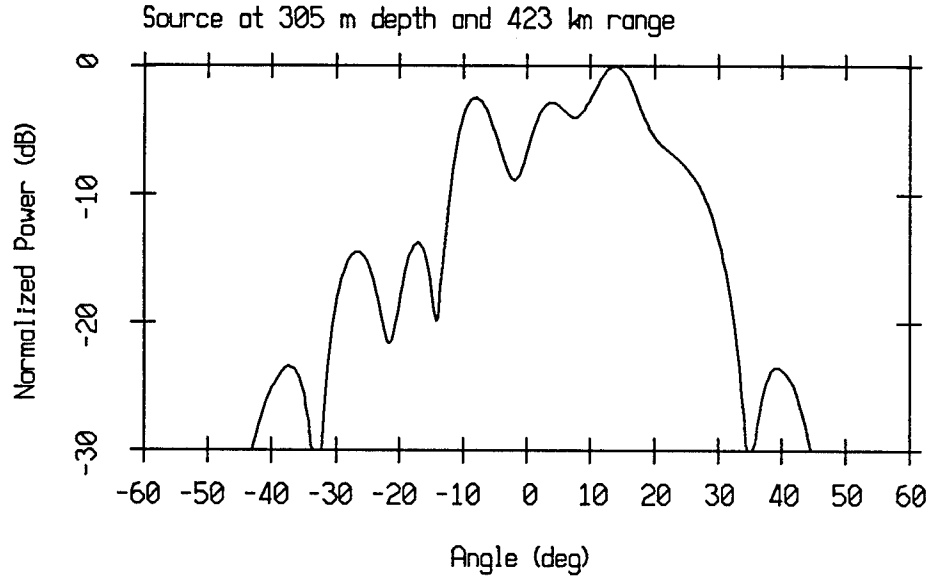
Source at 305 m depth and 423 km range
Normalized Power (dB)
0
-10
-20
-30
-60 -50 -40 -30 -20 -10 0 10 20 30 40 50 60
Angle (deg)

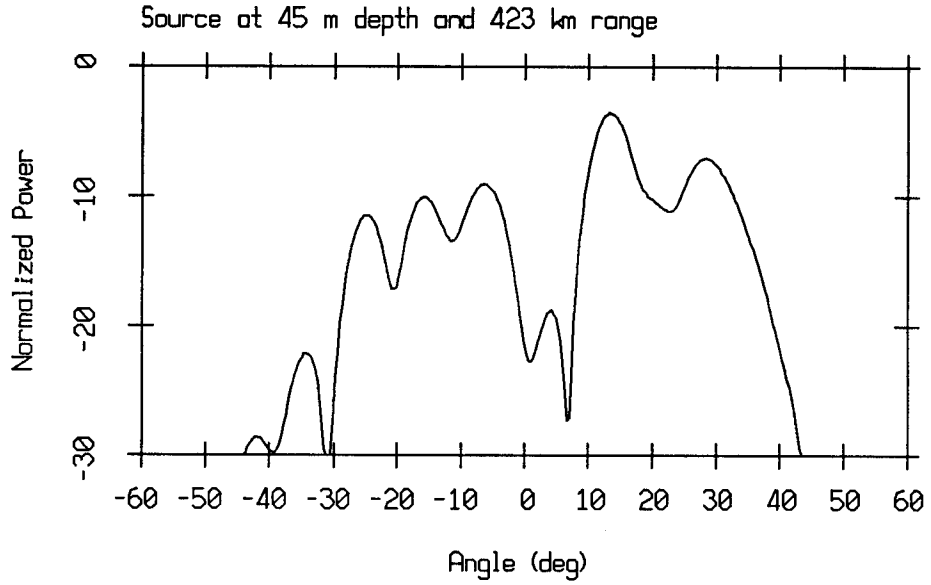
Source at 45 m depth and 423 km range
Normalized Power
0
-10
-20
-30
-60 -50 -40 -30 -20 -10 0 10 20 30 40 50 60
Angle (deg)

Source at 45 m depth and 423 km range
1000 m array with 12.353 m interelement spacing

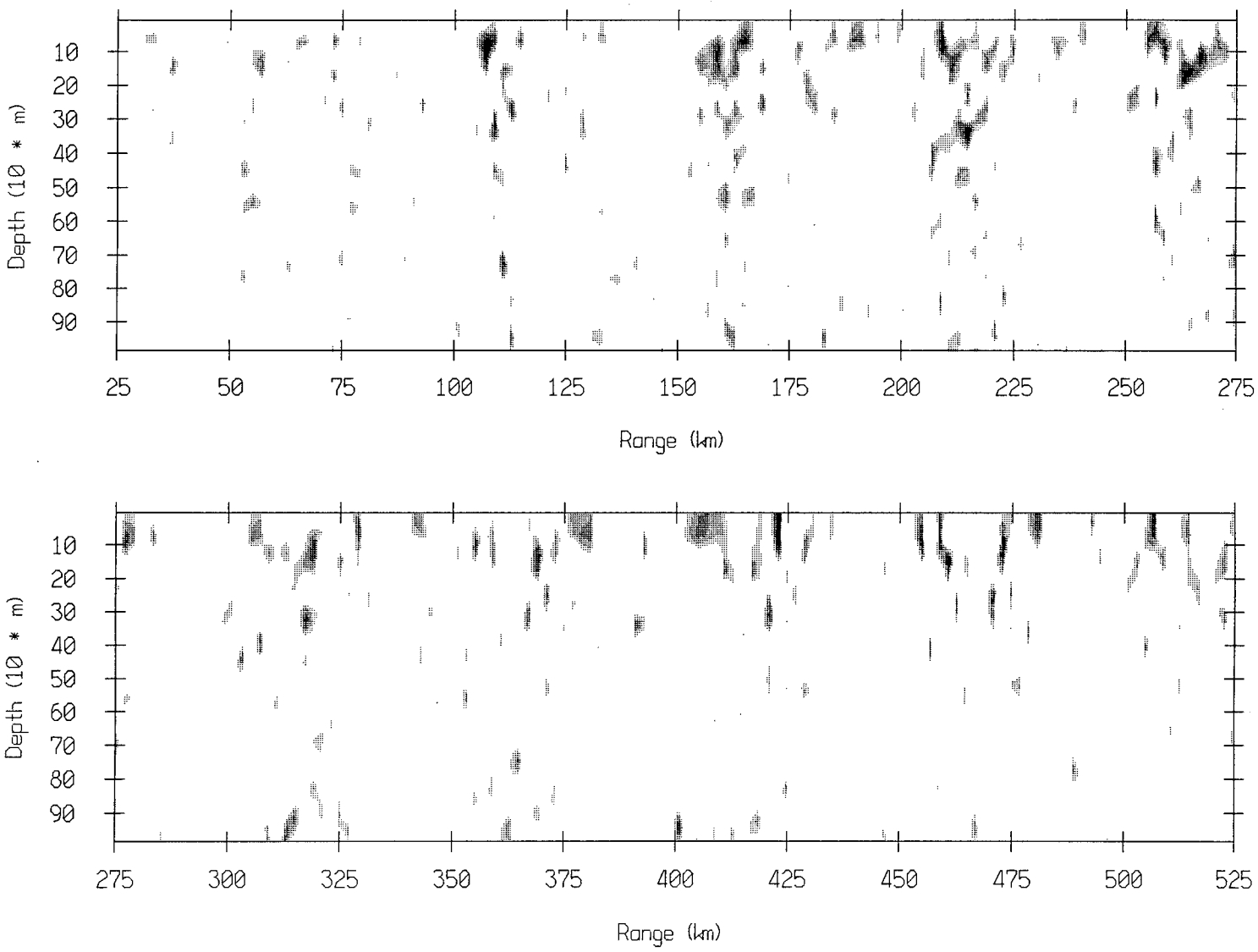

Source at 305 m depth and 423 km range
1000 m array with 12.353 m interelement spacing

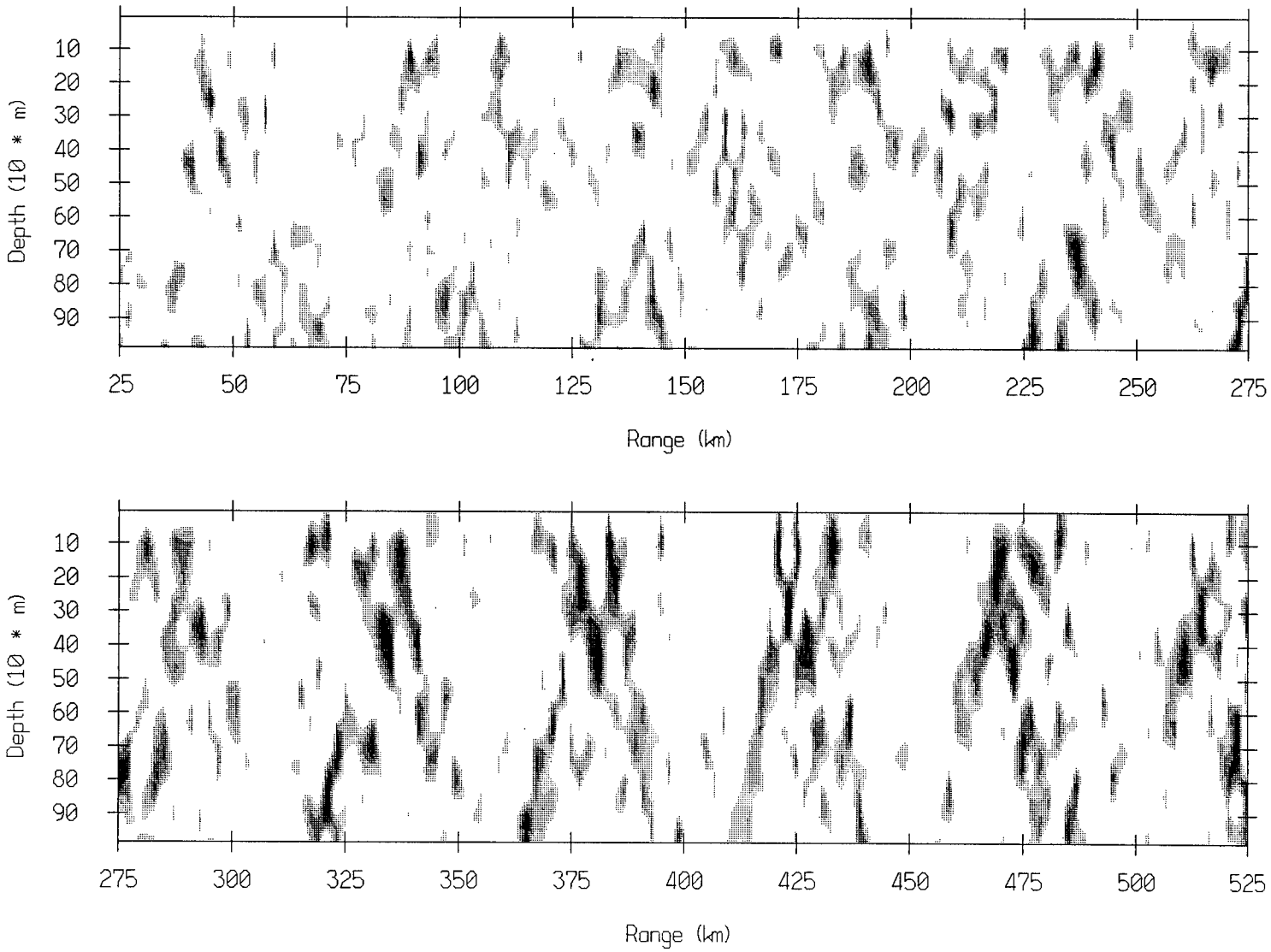

Source out of the MFP window at 45 m depth
4000 m array with 12.353 m interelement spacing
Shallow water sector

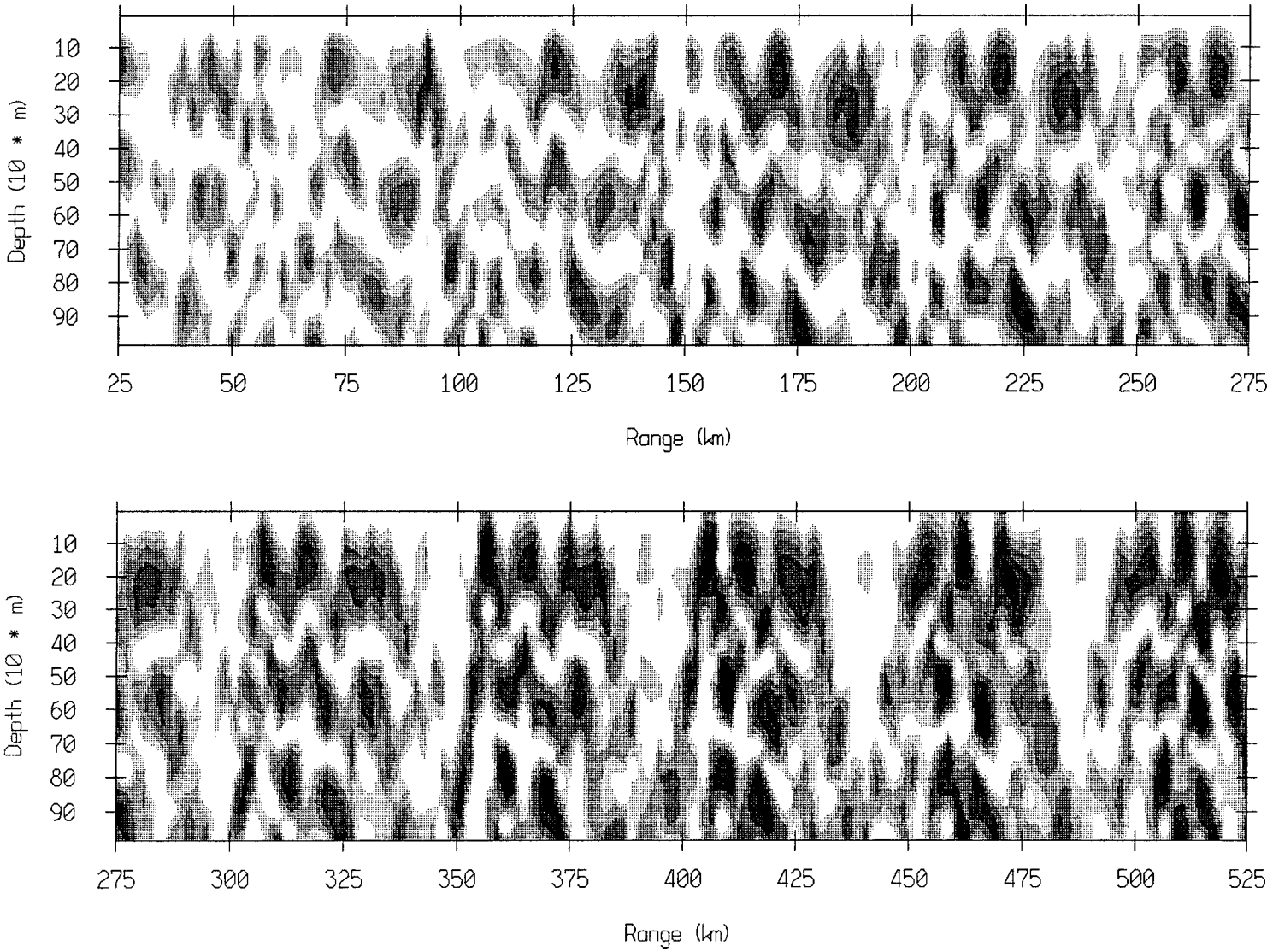

Source out of the MFP window at 45 m depth
4000 m array with 12.353 m interelement spacing
Small slope sector

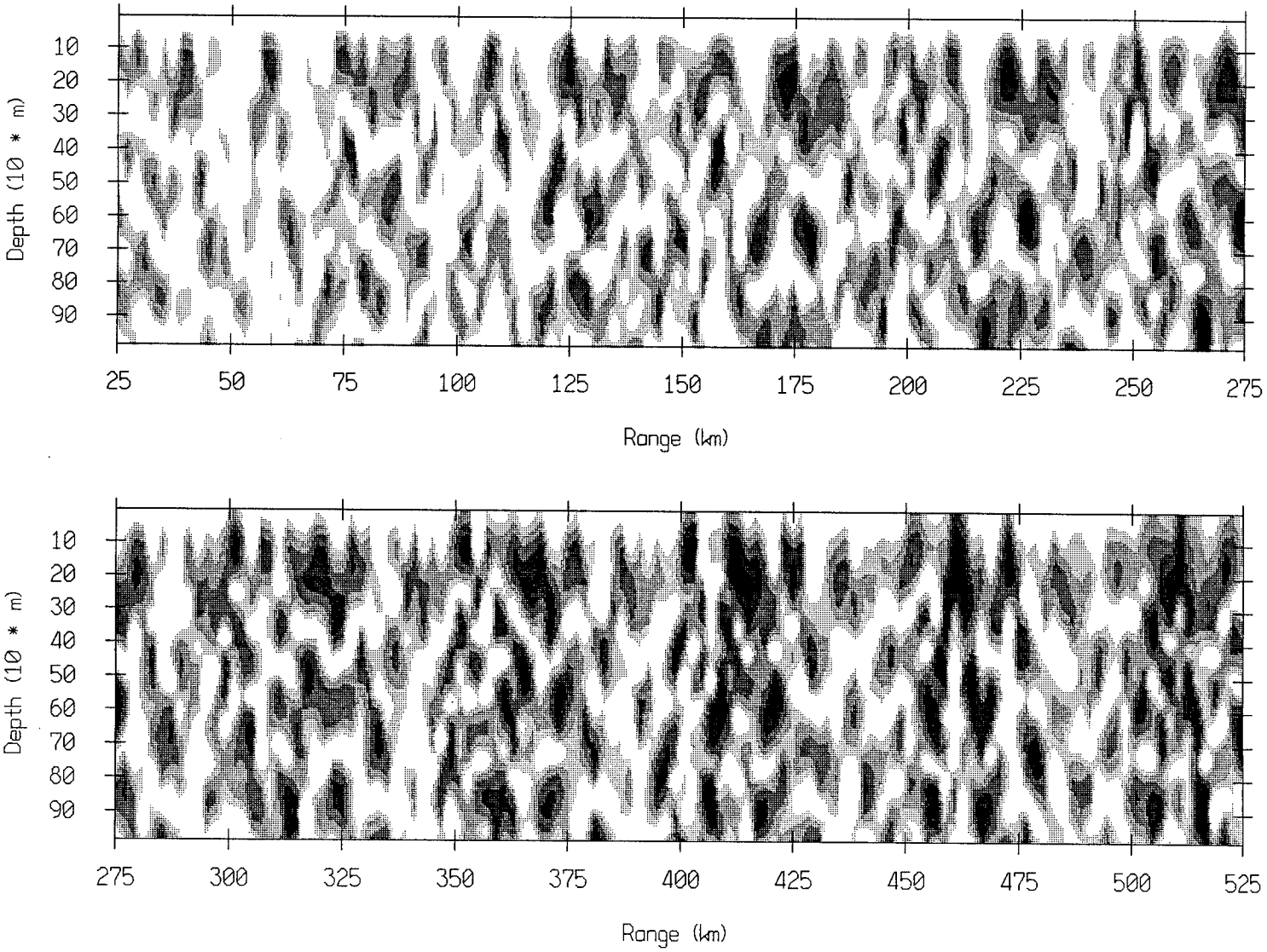

Source out of the MFP window at 45 m depth
4000 m array with 12.353 m interelement spacing
Steep slope sector

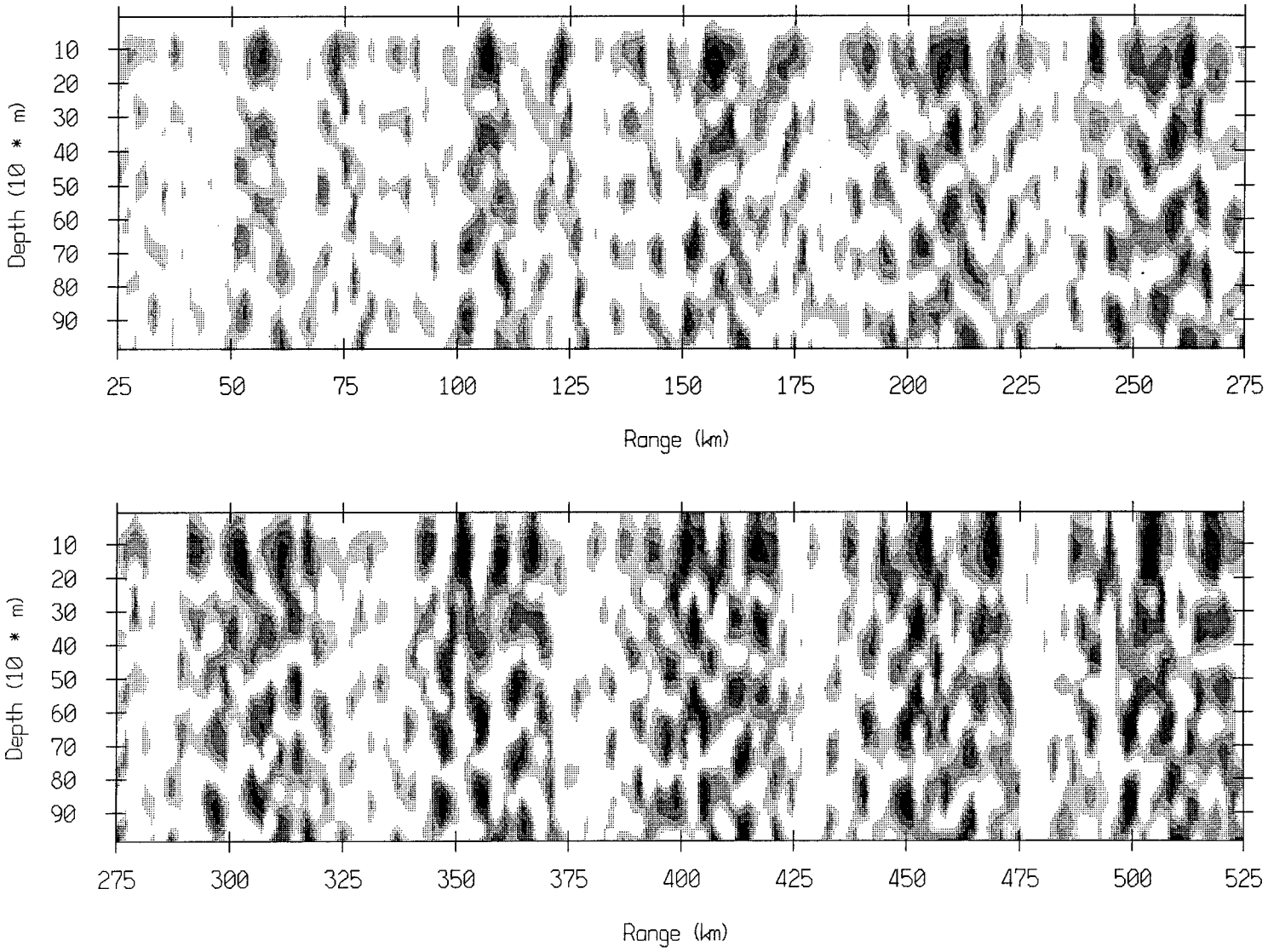

Source out of the MFP window at 45 m depth
4000 m array with 12.353 m interelement spacing
Gentle slope sector

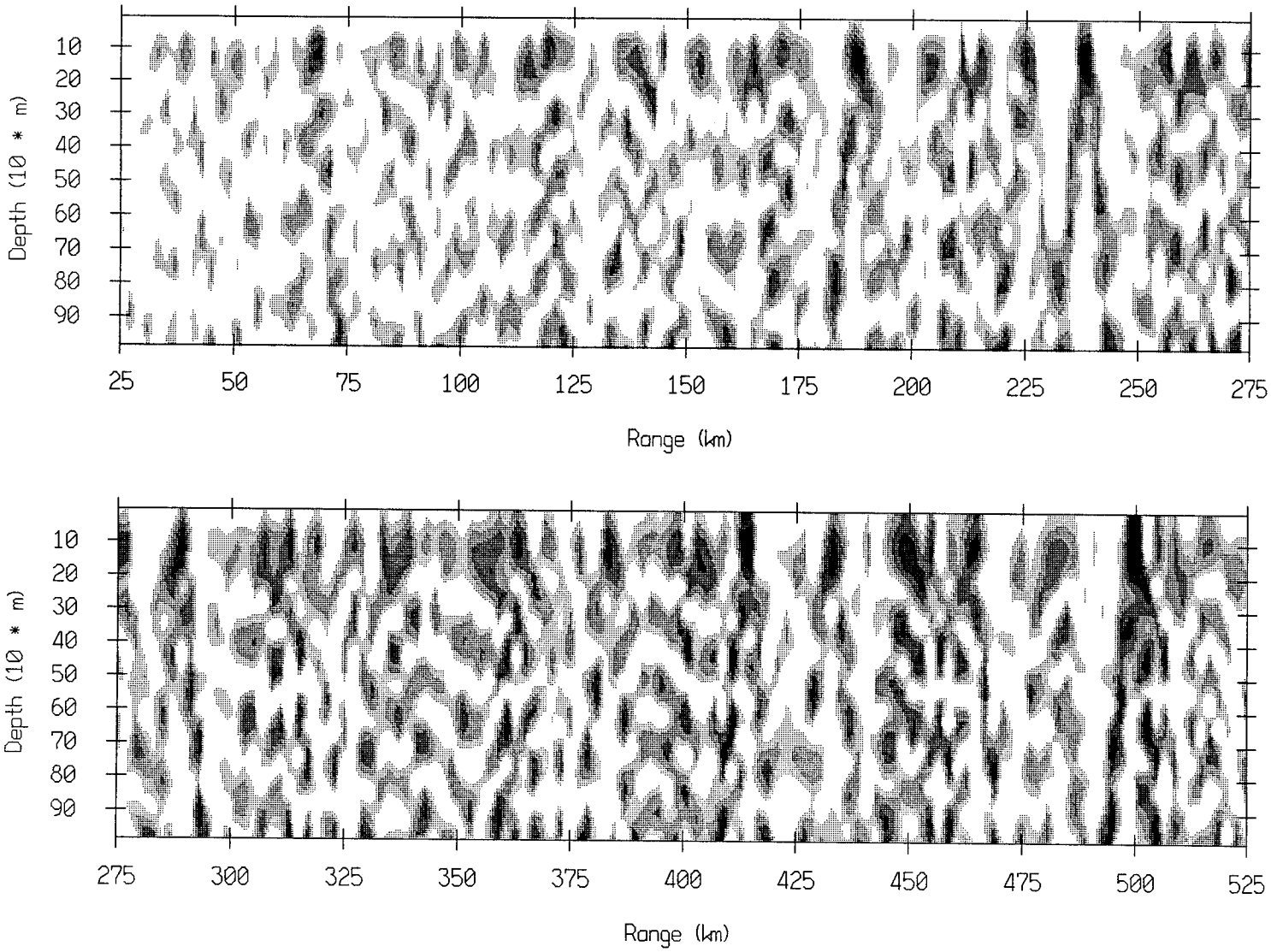

Source out of the MFP window at 45 m depth
4000 m array with 12.353 m interelement spacing
Shallow water sector
Surface normalized to highest peak

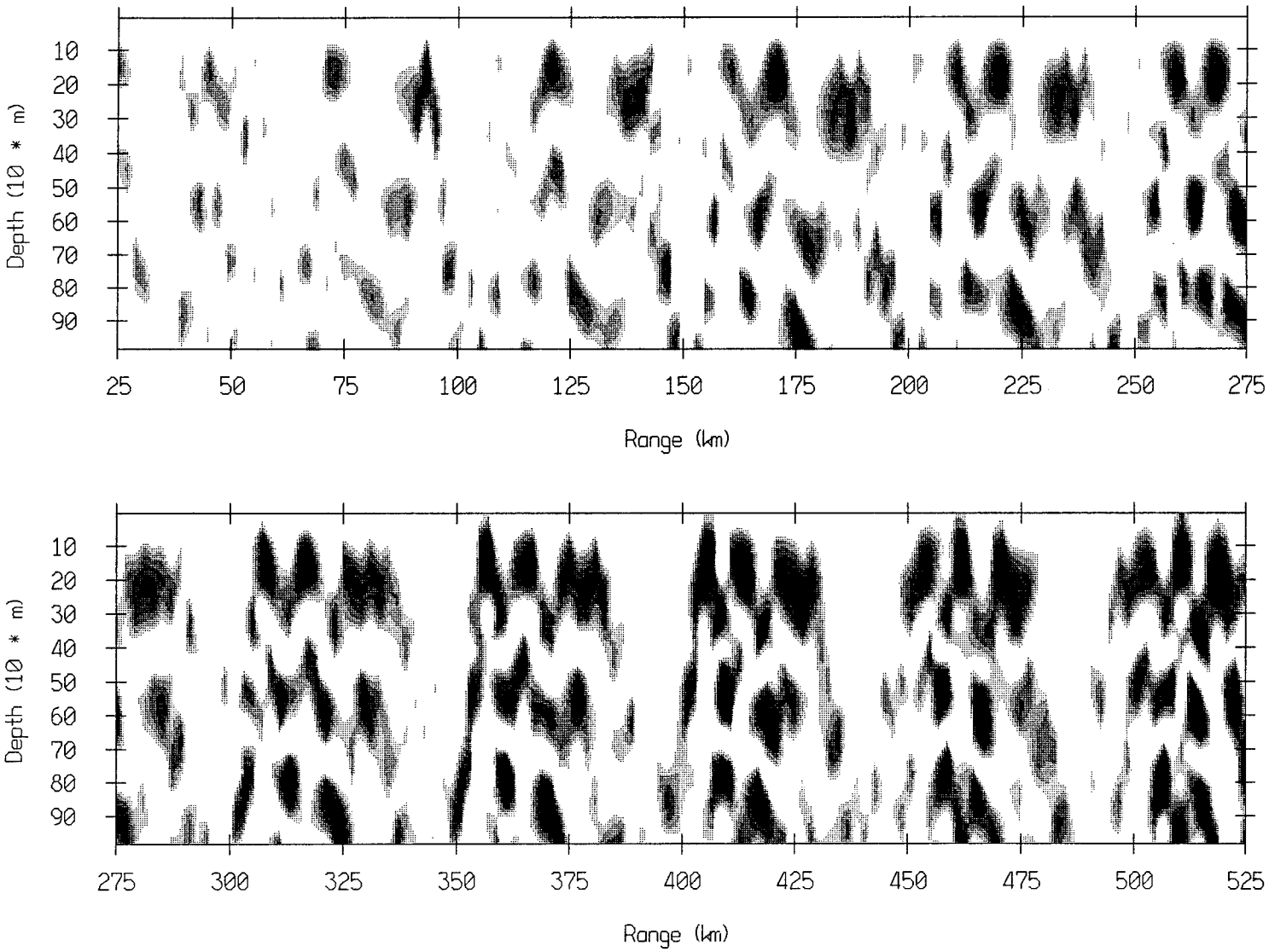

Source out of the MFP window at 45 m depth
4000 m array with 12.353 m interelement spacing
Small slope sector
Surface normalized to highest peak

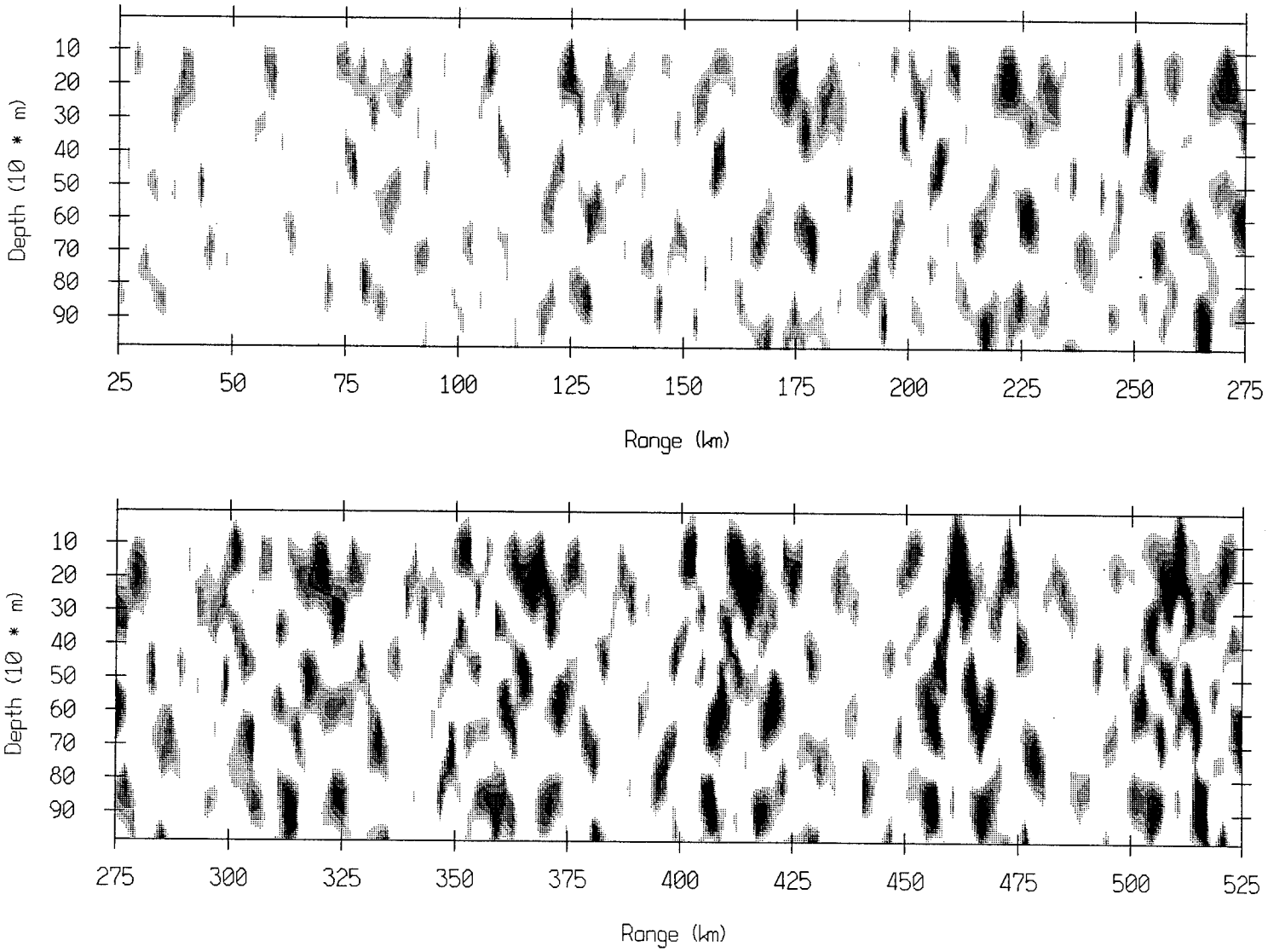

Source out of the MFP window at 45 m depth
4000 m array with 12.353 m interelement spacing
Steep slope sector
Surface normalized to highest peak

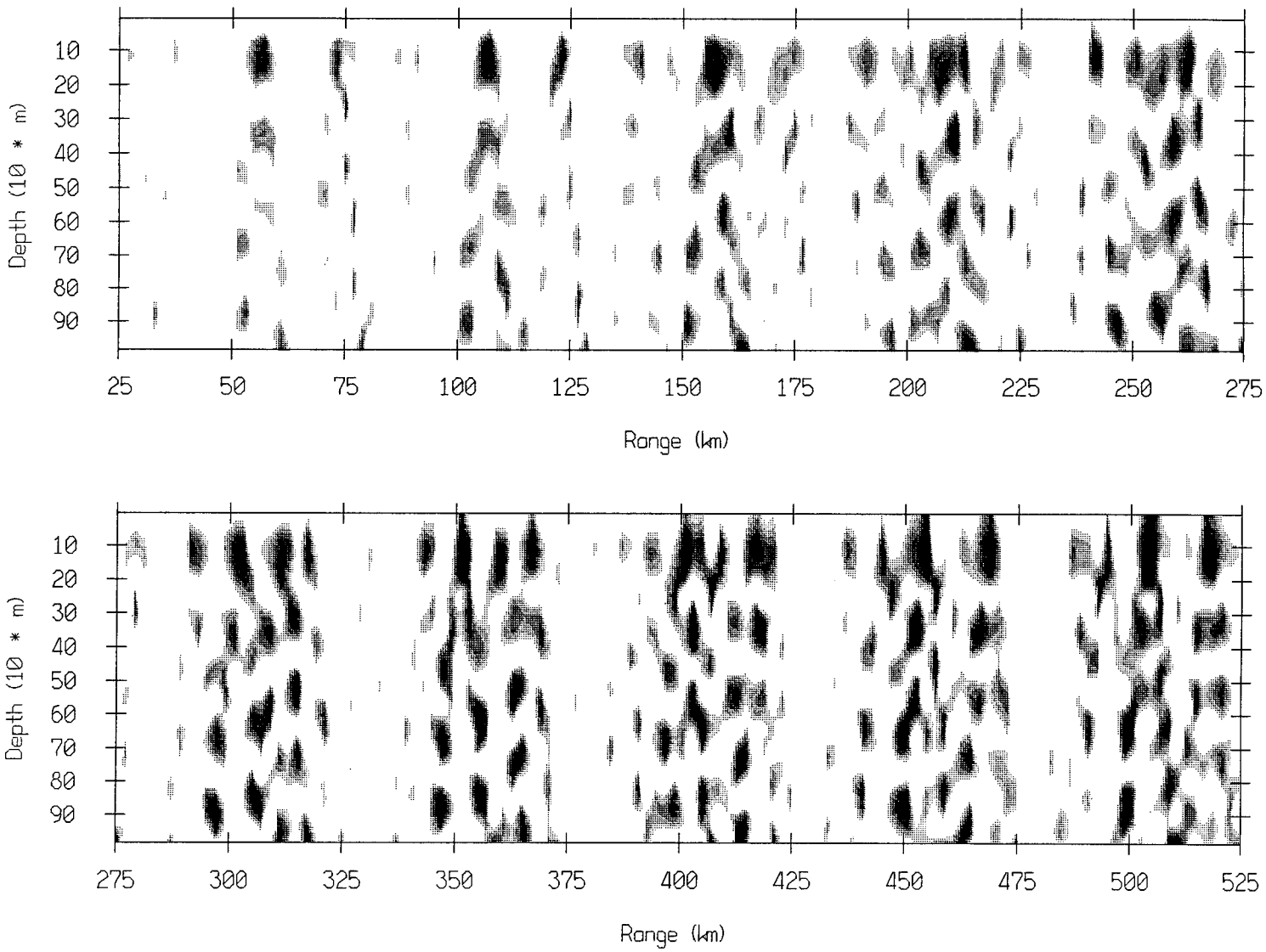

Source out of the MFP window at 45 m depth
4000 m array with 12.353 m interelement spacing
Gentle slope sector
Surface normalized to highest peak

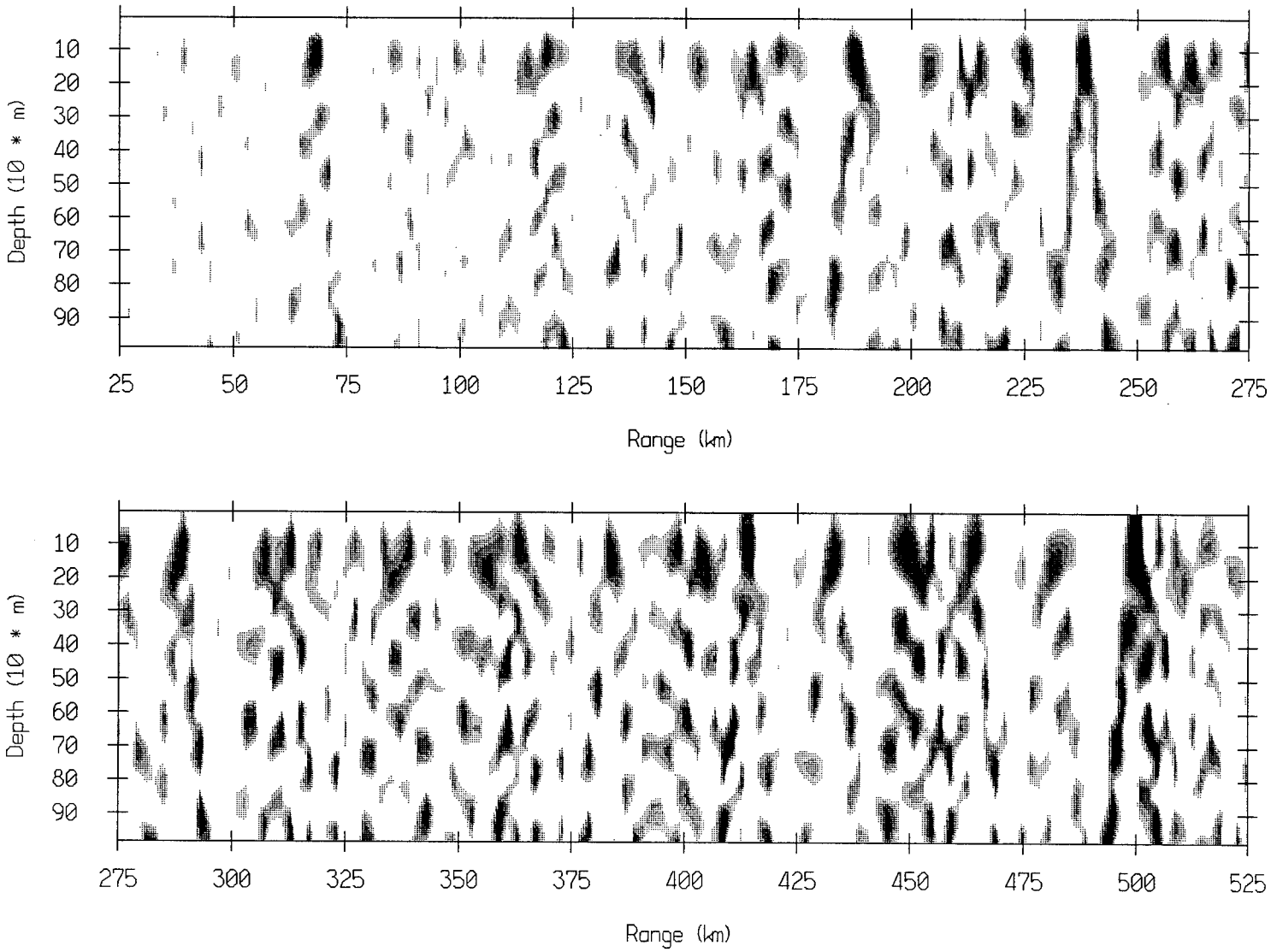

Source at 45 m depth and 423 km range
4000 m array with 12.353 m interelement spacing

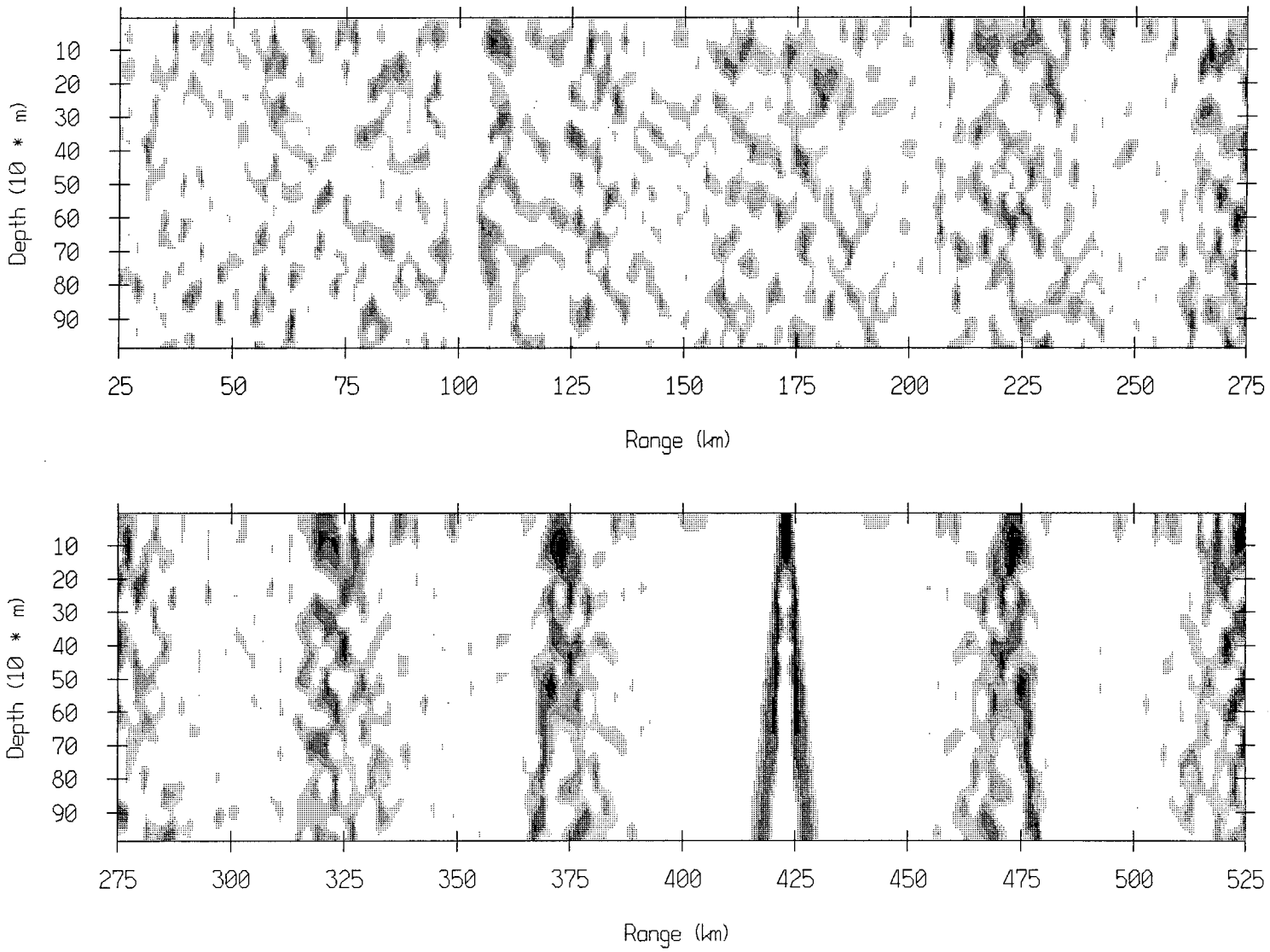

Source at 305 m depth and 423 km range
4000 m array with 12.353 m interelement spacing

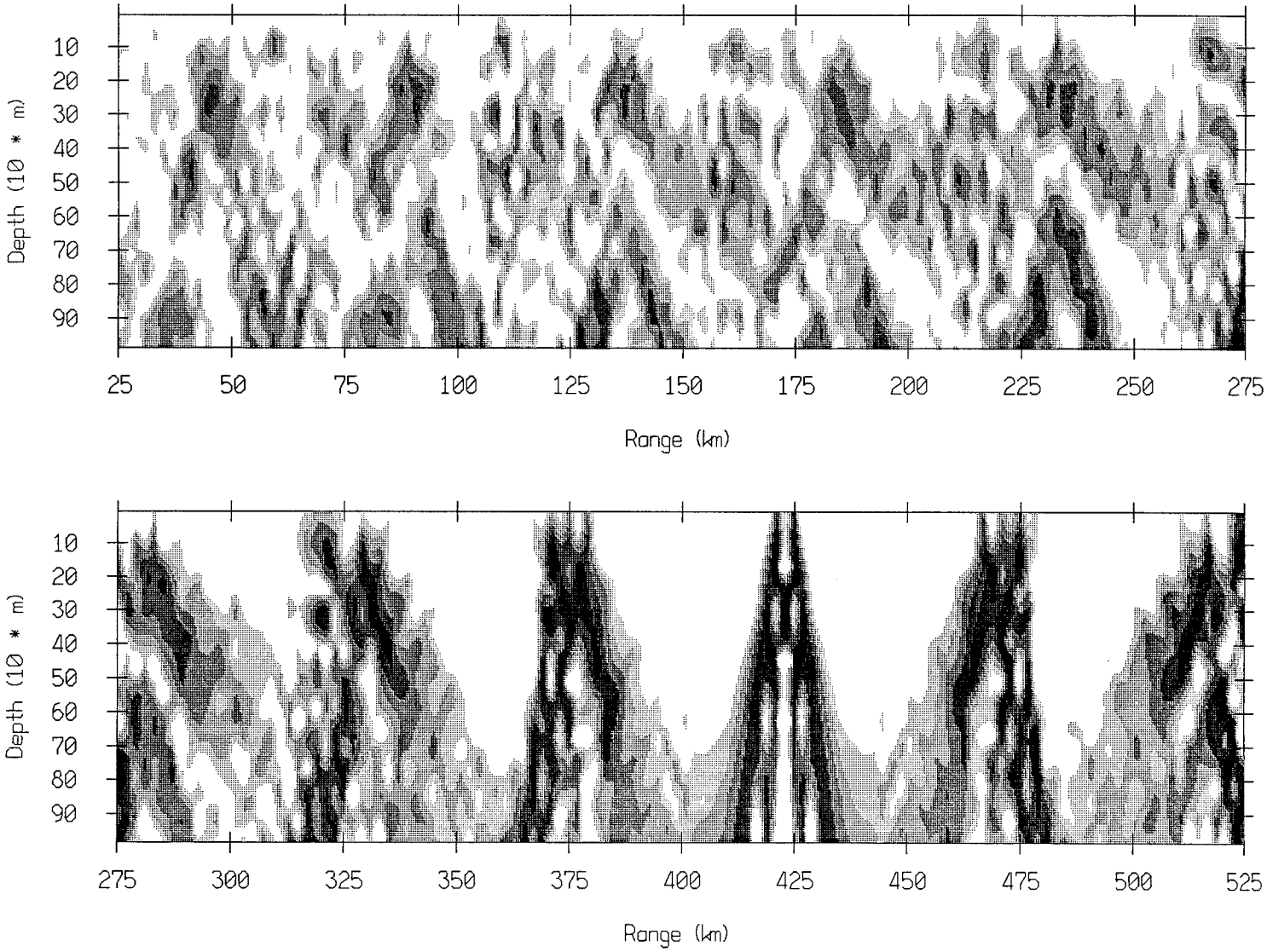

Source out of the MFP window at 45 m depth
4000 m array with 12.353 m interelement spacing
Shallow water sector

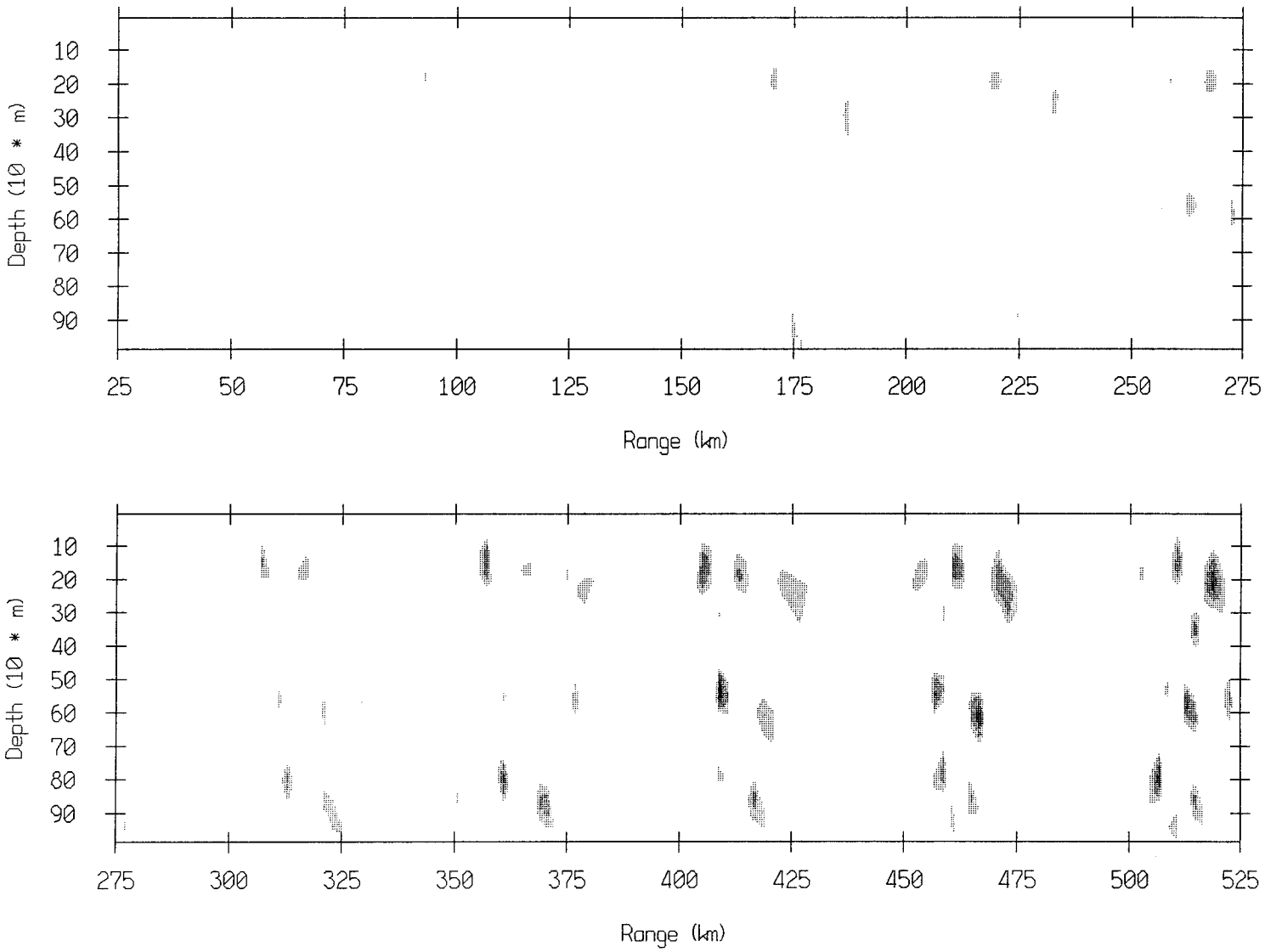

Source out of the MFP window at 45 m depth
4000 m array with 12.353 m interelement spacing
Small slope sector

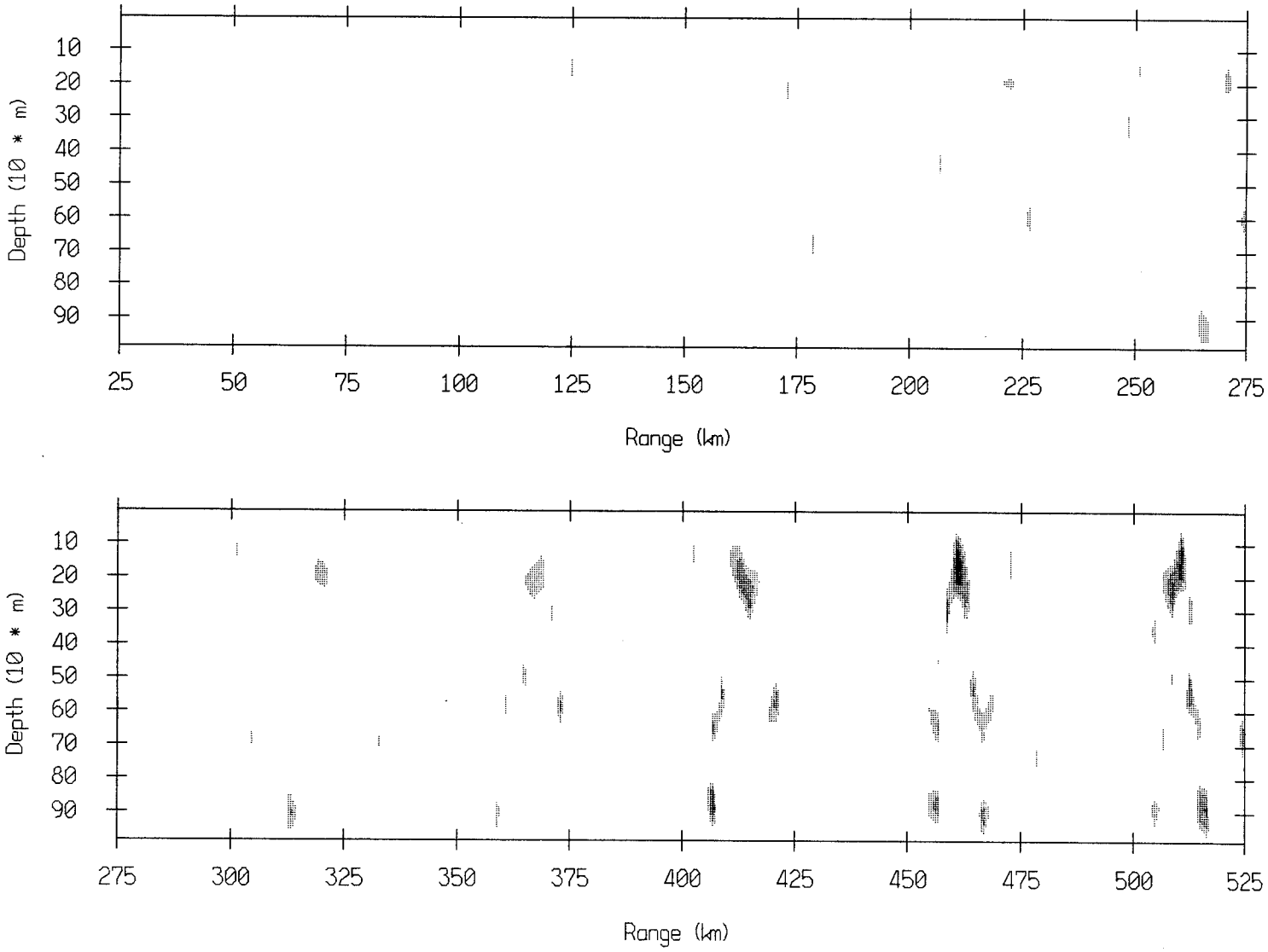

Source out of the MFP window at 45 m depth
4000 m array with 12.353 m interelement spacing
Steep slope sector

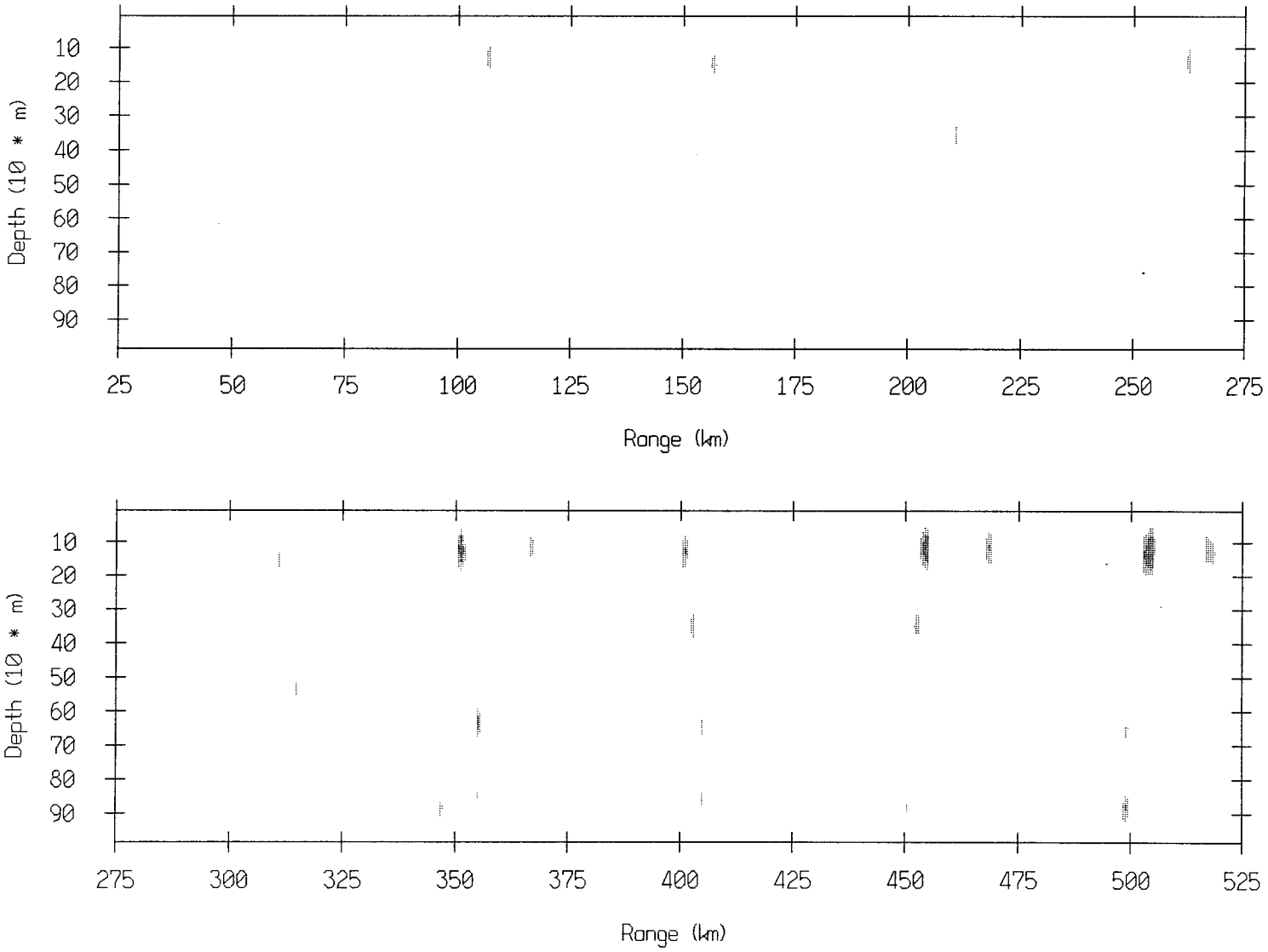

Source out of the MFP window at 45 m depth
4000 m array with 12.353 m interelement spacing
Gentle slope sector

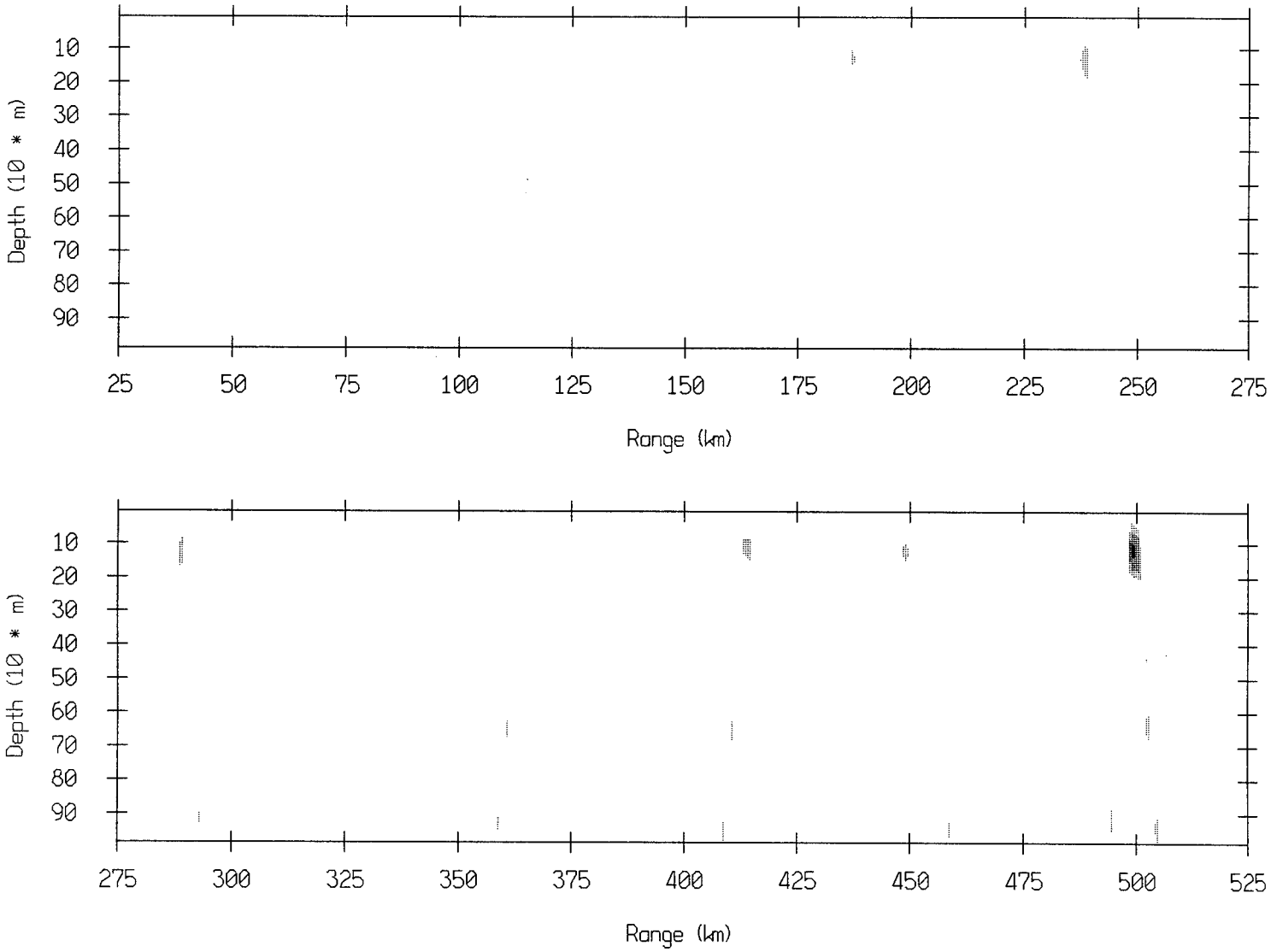

Source at 45 m depth and 423 km range
4000 m array with 12.353 m interelement spacing

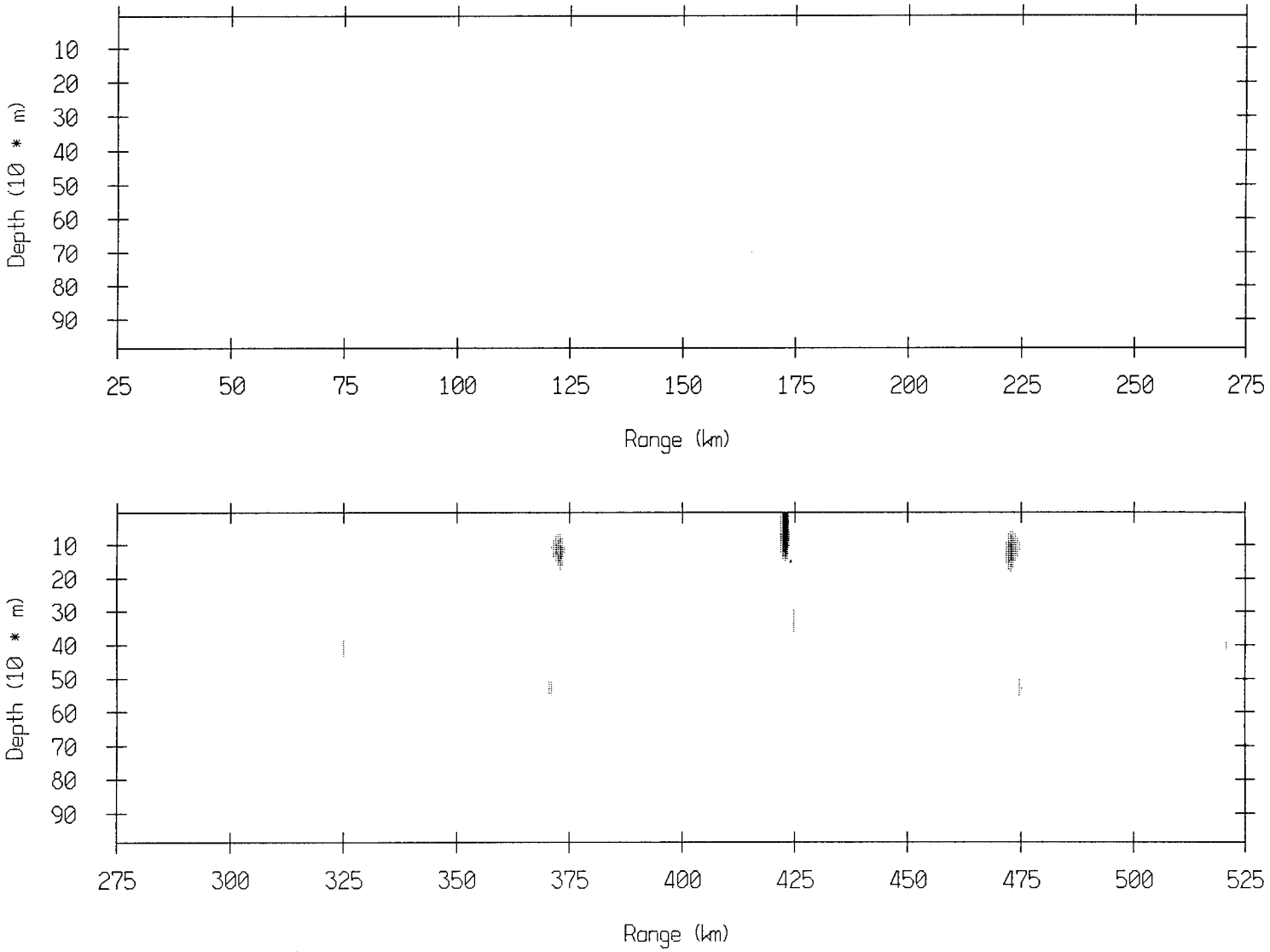

Source at 305 m depth and 423 km range
4000 m array with 12.353 m interelement spacing

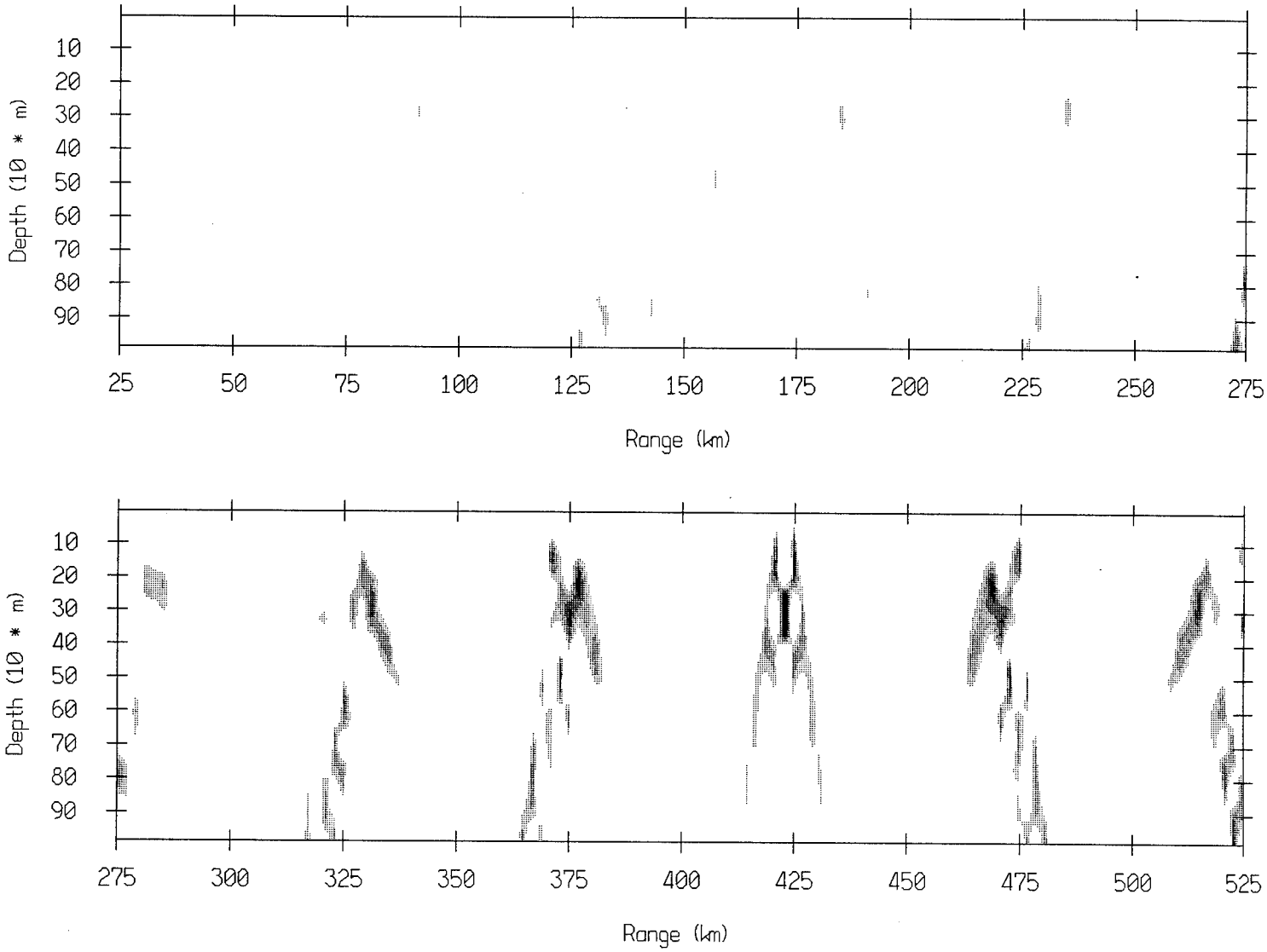

ONR/MPL REPORT DISTRIBUTION

Office of Naval Research (3)
Department of the Navy
Ballston Tower One
800 North Quincy Street
Arlington, VA 22217-5660
Atten: Dr. Mohsen Badiey
Code 3240A

Administrative Grants Officer (1)
Office of Naval Research
Resident Representative
University of California, San Diego, 0234
8603 La Jolla Shores Drive
San Diego, CA 92093-0234

Commanding Officer (2)
Naval Research Laboratory
Atten: Code 2627
Washington, D.C. 20375-5320

Defense Technical Information Center (4)
Building 5, Cameron Station
Alexandria, VA 22304-6145